

UNIVERSITY OF HAWAII LIBRARY

A TECHNIQUE FOR ESTIMATING  
TROPICAL OPEN OCEAN RAINFALL FROM  
SATELLITE OBSERVATIONS

A THESIS SUBMITTED TO THE GRADUATE DIVISION OF THE  
UNIVERSITY OF HAWAII IN PARTIAL FULFILLMENT  
OF THE REQUIREMENTS FOR THE DEGREE OF

MASTER OF SCIENCE  
IN METEOROLOGY  
DECEMBER 1974

By

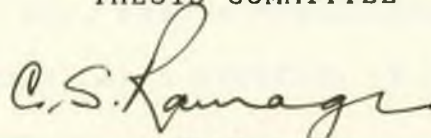
Bernard John Kilonsky

Thesis Committee:

Colin S. Ramage, Chairman  
Wan-Cheng Chiu  
James C. Sadler

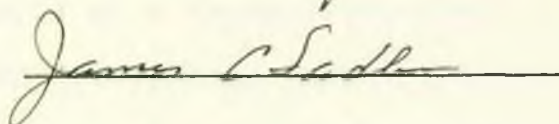
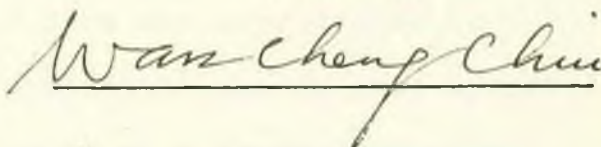
We certify that we have read this thesis and that in our opinion it is satisfactory in scope and quality as a thesis for the degree of Master of Science in Meteorology.

## THESIS COMMITTEE



---

Chairman



## ABSTRACT

The purpose of the study was to obtain accurate estimates of tropical open ocean rainfall from satellite observations.

The approach used was the development of a procedure for extracting (approximately one month of data per person per week) highly reflective clouds from visual satellite pictures and mosaics. The project was visualized as a frequency study. That is, for a day, either significant highly reflective cloud was observed at a location or significant cloud was not observed.

The rapid extraction of data was expected to be produced by fitting highly reflective clouds into standard shapes (circles, ellipses, etc.) on a transparent overlay. The National Oceanographic and Atmospheric Administration (NOAA) cloud mosaics were examined and it was determined that almost all desired cloud masses could be defined by a combination of six circles, seven wide ellipses with four orientations, and eight narrow ellipses with four orientations. The transparent overlays were drafted and fitted to the grid size of the mosaic, and a computer program was compiled to transform data from the selected standard shape to the correct position in a data array.

The month of August 1972 was examined in the formative

stages of this project. Control studies were conducted using the data collection scheme. These studies supported the validity of the approach and the consistency of the method.

The highly reflective clouds for the period between May 1971 and January 1974 were compiled and statistically tested for a regression relationship. A group of 820 coral island monthly rainfall observations were used as a sample. The correlation coefficient using highly reflective cloud cover as the predictor and rainfall as the predictand was .75. The line of regression passed near the origin and was equidistant from the abscissa and ordinate. The F calculated from an analysis of variance table was highly significant on the 1% level. Thus, the amassed charts and cross sections of highly reflective clouds were found useful in estimating the rainfall for the period from May 1971 to January 1974.

## TABLE OF CONTENTS

ABSTRACT. . . . .	iii
LIST OF TABLES. . . . .	vi
LIST OF FIGURES . . . . .	vii
INTRODUCTION. . . . .	1
DEVELOPMENT OF THE DATA COLLECTION SCHEME . . . . .	2
INITIAL RAINFALL CORRELATION. . . . .	6
EL-NINO DATA COLLECTION . . . . .	12
FINAL RAINFALL CORRELATION. . . . .	18
CONCLUSION AND DISCUSSION . . . . .	23
APPENDIX. . . . .	79
REFERENCES. . . . .	82

## LIST OF TABLES

Table		Page
1	An analysis of variance table for testing the significance of the regression relationship for the initial equation predicting rainfall from highly reflective cloud. . . . .	9
2	An analysis of variance table for testing the significance of the correlation coefficient for the initial equation predicting rainfall from highly reflective cloud. . . . .	10
3	An analysis of variance table for testing the significance of the regression relationship for the final equation predicting rainfall from highly reflective cloud. . . . .	19
4	An analysis of variance table for testing the significance of the correlation coefficient for the final equation predicting rainfall from highly reflective cloud. . . . .	19
5	An analysis of variance table for testing the significance of the regression relationship for the equation predicting rainfall from cloud cover in oktas. . . . .	21
6	An analysis of variance table for testing the significance of the correlation coefficient for the equation predicting rainfall from cloud cover in oktas. . . . .	21

## LIST OF FIGURES

Figure		Page
1	Original draft of the six circles, seven wide ellipses, and eight narrow ellipses . . . . .	32
2	Standard shape of orientation 2 and size 1 is correctly fitted to a highly reflective cloud mass on a NOAA digitized cloud mosaic. . . . .	33
3	Shape 03 as it appears in a one degree grid mapping one and two days of highly reflective cloud cover . . . . .	34
4	Shapes 54 to 84 mapped at the same grid center point and limited to a one unit per point per day incrementation. . . . .	35
5	Average cloud cover in oktas for the period August 11, 1972, to August 20, 1972 from 20°N to 20°S and from 155°E to 80°W in a two and one half degree grid. . . . .	36
6	Average cloud cover in oktas for the month of August 1972 from 20°N to 20°S and from 155°E to 80°W in a two and one half degree grid. . . . .	37
7	Part of the hand-analyzed computer printout that maps the area from 20°N to 20°S and from 155°E to 80°W in a one degree grid for the ten day period between August 11, 1972, and August 20, 1972 . . . . .	38
8	Part of the hand-analyzed computer printout that maps the area from 20°N to 20°S and from 155°E to 80°W in a one degree grid for the month of August 1972 . . . . .	39

9	Statistics and scatter diagram derived from equations (2.1) to (2.7) for the month of August 1972 . . . . .	41
10	Part of the hand-analyzed computer printout that maps the area from 20°N to 20°S and from 125°E to 80°W in the Northern Hemisphere and 150°E to 80°W in the Southern Hemisphere for the month of August 1972 . . . . .	42
11	Part of the hand-analyzed computer printout that maps the area from 20°N to 20°S and from 125°E to 80°W in the Northern Hemisphere and 150°E to 80°W in the Southern Hemisphere for the period May 1972 minus May 1973 . . . . .	43
12	Cross section, 20°N to 20°S, plotting the sum of the total number of days of highly reflective cloud cover for the month of August 1972 from 125°E to 80°W in the Northern Hemisphere and 150°E to 80°W in the Southern Hemisphere. . . . .	45
13	Cross section, 20°N to 20°S, plotting the sum of the total number of days of highly reflective cloud cover for forty degree increments of the Pacific Ocean region for the month of August 1972. . . . .	47
14	Cross section, 20°N to 20°S, plotting the average number of days of highly reflective cloud cover for the month of May 1972 from 125°E to 80°W in the Northern Hemisphere and from 150°E to 80°W in the Southern Hemisphere. . . . .	49
15	Cross section, 20°N to 20°S, plotting the average number of days of highly reflective cloud cover for the month of May 1972 from 161°E to 160°W . . . . .	51
16	Cross section, 20°N to 20°S, plotting the average number of days of highly reflective cloud cover for the month of May 1972 from 139°W to 120°W . . . . .	53



17	Cross section, 20°N to 20°S, plotting the average number of days of highly reflective cloud cover for the month of May 1972 from 119°W to 115°W . . . . .	55
18	Cross sections, 20°N to 20°S, plotting the average number of days of highly reflective cloud cover for forty degree increments of the Pacific Ocean region for the month of May 1972. . . . .	57
19	Cross sections, 20°N to 20°S, plotting the average number of days of highly reflective cloud cover for twenty degree increments of the Pacific Ocean region for the month of May 1972 . . . . .	59
20	Cross sections, 20°N to 20°S, plotting the average number of days of highly reflective cloud cover for selected five degree latitude strips. . . . .	60
21	Average number of days of highly reflective cloud cover between 20°N and 5°N, 5°N and 5°S, 5°S and 20°S, 20°N and 20°S listed and plotted from 125°E to 170°E or 150°E to 170°E . . . . .	62
22	Number of days of highly reflective cloud cover at 10°S, 5°S, the equator, and 5°N listed and plotted from 125°E to 170°E or 150°E to 170°E. . . . .	64
23	Cross section, 20°N to 20°S, plotting the sum of the differences in the number of days of highly reflective cloud cover for May 1972 minus May 1971. . . . .	66
24	Cross section, 20°N to 20°S, plotting the sum of the differences in the number of days of highly reflective cloud cover for May 1972 minus May 1971 for forty degree increments of the Pacific Ocean region . . . . .	68
25	Cross section, 20°N to 20°S, plotting the difference in the average number of days of highly reflective cloud cover for May 1972 minus May 1971 from 161°E to 160°W . . . . .	70

26	Statistics and scatter diagram derived from equations (2.1) to (2.7) for the regression line fitting rainfall to highly reflective cloud. . . . .	72
27	Statistics and scatter diagram derived from equations (2.1) to (2.7) for the regression line fitting rainfall to cloud cover in oktas . . . . .	74
28	Cross section, 20°N to 20°S, plotting five estimations of the annual precipitation in centimeters for the Pacific Ocean region . . . . .	76
29	Cross section, 20°N to 20°S, showing the annual precipitation in centimeters for the Pacific Ocean. Three periods are shown; May 1971 to April 1972, May 1972 to April 1973, and a 12 month extrapolation of May 1973 to January 1974. . . . .	78

## CHAPTER I

### INTRODUCTION

Rainfall over most of the tropical oceans has been an unmeasurable quantity. The purpose of this study was to develop accurate long term estimates of tropical open ocean rainfall. A scheme that permitted the rapid extraction of highly reflective cloud masses from visual satellite pictures and mosaics was proposed. It eliminated the necessity of examining every square degree while mapping these cloud masses in a one degree grid. Thus, the study resolved itself into four major processes. First, the data collection scheme was developed and verified. Second, a pilot study was conducted and the cloud masses statistically tested for rainfall correlation. Third, the basic data collection was compiled, and a program developed to produce more usable data formats. Fourth, this long term data collection was statistically tested for rainfall correlation.

At the onset of this study, it was hoped that the rainfall estimates could be published as an atlas. However, the vast quantity of the data precluded this. Thus, this report limits itself to examples of the formats in which the rainfall estimates are available.

## CHAPTER II

## DEVELOPMENT OF THE DATA COLLECTION SCHEME

The construction of the data collection scheme incorporated four major procedures. The first was the selection of the type of cloud mass to be mapped. The second, the drafting of the standard shapes that were chosen to define the areas of these cloud masses. The third, the compilation and verification of a computer program that mapped the area enclosed in the standard shape to its corresponding points in a one degree grid. The fourth, the definition and evaluation of the subjective fitting of the standard shape to the selected cloud mass.

Most rainfall in the tropics is caused by organized convection (Riehl, 1954). As the end result of the study was to develop an accurate rainfall estimate, it was thought that this could be achieved by limiting the study to relatively large scale convective activity. Thus, the data input was confined to what appeared on the NOAA digitized cloud mosaics as highly reflective cloud masses with a radius equal to or greater than two degrees.

These highly reflective cloud masses were carefully examined on the NOAA mosaics and on the output from the Defense Meteorology Satellite Program (DMSP) and the most useful shapes for both data sources were drafted in the

form of a transparent overlay (see Fig. 1). These overlays were then fitted by visually mapping the one degree intersections on the NOAA mosaics that were included in the shapes when their centers were placed at a preselected latitude and longitude. In this way each shape's area was defined relative to its midpoint. The final mapped area of each shape was made slightly smaller than the shape itself; this allowed the cloud mass of interest to be completely enclosed within the chosen shape. A seven digit number was used to identify the selected shape and its midpoint. The left-most two digits described the orientation and size of the shape, the next two digits the row position of the center point of the shape, and the next three digits the column position of this center point (see Fig. 2).

A computer program was developed that increased the integer values of the enclosed grid points by one unit for each day those points were covered by highly reflective cloud (see Fig. 3). Because of the efficiency of the DO loop in Fortran programming, this technique was used to direct the additive incrementation. Overlapping of the shapes used to describe a cloud mass was permitted by limiting the incrementation to one unit per point per day (see Fig. 4). Thus, the grid could have been printed without any further calculation in units of the number of days of highly reflective cloud per selected time period. If percent coverage was desired, the number of days covered

was divided by the total number of days included. Thus, the total number of days or the percentage of days covered by the highly reflective cloud was readily obtainable for any desired time period.

At this stage each shape was centered at a selected point in the grid, and the computed output was verified to be accurate in position and area. Each shape was then overlapped with other shapes and the output checked for accuracy and representativeness. Numerous space and time combinations of input data were also computed and the output array checked to verify the accuracy of the transformations.

A pilot study was then conducted to evaluate the data collection scheme in a real situation. The area from  $20^{\circ}\text{N}$  to  $20^{\circ}\text{S}$  and  $155^{\circ}\text{E}$  to  $80^{\circ}\text{W}$  in the month of August 1972 was examined. Using the proposed data collection scheme, two sets of unanalyzed charts showing the number of days of highly reflective cloud cover for ten day periods and for the complete month were independently assembled by two graduate students. The students hand-analyzed their charts, and these two sets were then visually compared. No significant areal or quantitative differences were apparent in either the ten day or monthly totals.

Using a method developed by Sadler (1969), the author, in a previous study, had compiled charts for August 1972 that mapped the ten day and monthly averages of total cloud

in oktas in a two and one half degree grid. Comparisons of the ten day and monthly totals of the number of days of highly reflective cloud cover and the ten day and monthly averages of cloud cover in oktas showed good agreement in the definition of the geographic extent of their measured fields (see Figs. 5-8). Although the comparison between Sadler's and our method verified that our computed output was a mapping of existent cloud cover, it must be emphasized that the two methods are intrinsically different. The oktas method was the average of the daily cloud cover and included all types of cloud as input data. Our method was a frequency study and was limited to what was interpreted as significant rain producing cloud.

### CHAPTER III

#### INITIAL RAINFALL CORRELATION

In any study that attempts to use satellite derived data to estimate rainfall, the calibration of this data in terms of the dependent variable (rainfall) remains the most demanding aspect of the problem. As rainfall is not routinely measured on ships, the only available sources of rainfall measurements in the Pacific Ocean region are island stations. Since this study was an attempt to estimate open ocean rainfall, the orographic effects of these islands on the rainfall totals had to be eliminated. To this end, the rainfall observations were limited to coral islands that were less than one hundred feet in elevation (see Appendix). A set of monthly total rainfall observations from thirty-five islands was compiled for the month of August 1972 and used as the dependent variable, X2. The monthly highly reflective cloud totals at the exact geographic position of the respective stations were listed as the independent variable, X1. Assuming a linear relationship between X1 and X2, the theory of least squares was used to fit a line of regression that yielded predicted values of the dependent variable.

Besides the assumption of a linear relationship between X1 and X2, we also assumed that there was no relation



between successive pairs of observations; that is, where  $N$  was the total number of pairs in the sample the  $N$  observation pairs were assumed to be independent from each other. Another assumption was that the coral island rainfall statistics were truly representative of the open ocean rainfall. This may or may not have been a valid assumption. However, this set of data had to be used, as no other open ocean measurements of rainfall were available. It was thought that the limiting of the set to those coral islands below one hundred feet did help minimize the orographic effects of these islands on rainfall.

The basic equations used in the calculation of the regression relationship are listed in chapter four of Panofsky and Brier (1968). The line of regression  $X_2$  on  $X_1$  is given by:

$$X_2' = a + b_{2.1}(X_1) \quad (2.1)$$

$$b_{2.1} = \frac{N\sum X_1 X_2 - \sum X_1 \sum X_2}{N\sum X_1^2 - (\sum X_1)^2} \quad (2.2)$$

$$a = (\overline{X_2}) - b_{2.1}(\overline{X_1}) \quad (2.3)$$

The following notation was used in the above equations:

$b_{2.1}$  the slope of the line of regression defined by equation (2.2)

$a$  constant defined by equation (2.3)

- X2      the actual observations of the predictand, in this case, the monthly rainfall totals from coral island stations
- X2'     values of X2 given by the line of regression, in this case, the estimated rainfall
- X1      the actual observations of the predictor, in this case, the monthly totals of highly reflective cloud cover
- N        the total number of pairs in the sample
- $\Sigma$         the variables that follow this notation are summed over their range
- ( $\bar{\quad}$ )    the mean of the variable included in the parenthesis.

Other equations used in the study of the regression relationship include the standard deviation, S1 and S2, of both the independent and dependent variables given in chapter one of Panofsky and Brier (1968) as:

$$S1 = \sqrt{\frac{\Sigma X1^2}{N} - (\bar{X1})^2} \quad (2.4)$$

$$S2 = \sqrt{\frac{\Sigma X2^2}{N} - (\bar{X2})^2} \quad (2.5)$$

Equations to calculate the linear correlation coefficient, R12, and the scatter about the line of regression, S2.1, are listed in chapter four of Panofsky and Brier (1968) as:

$$R_{12} = b_{2.1}(S_1/S_2) \quad (2.6)$$

$$S_{2.1} = \sqrt{S_2^2 - b_{2.1}^2 S_1^2} \quad (2.7)$$

A computer program that calculated these statistics and plotted a scatter diagram that included the line of best fit was developed, and the rainfall and highly reflective cloud data for the month of August 1972 used as input (see Fig. 9). The results of this program were then used to construct an analysis of variance table for testing the significance of a regression relationship. (See, for example, Table 23 of Panofsky and Brier, 1968.)

Table 1

Analysis of Variance Table for  
Testing the Significance of a Regression Relationship

Source	SS	dof	MS	F
Total	575951.6	34	16949.4	
Slope of regression line	343553.6	1	343553.6	49.17
Deviations from regression	231282.2	33	7008.5	

The F shown in Table 1 was the ratio of mean squares, with the larger in the numerator. The significance level was determined from Table 19 of Panofsky and Brier (1968). The F found in Table 1 was highly significant. The 1% limit for one and thirty-three degrees of freedom (see

Table 19 of Panofsky and Brier, 1968) was 7.50 compared to the observed F of 49.17.

An analysis of variance table for testing the significance of the correlation coefficient was also constructed. (See, for example, Table 24 of Panofsky and Brier, 1968.)

Table 2

Analysis of Variance Table for  
Testing the Significance of the Correlation Coefficient

Source	SS1	dof	MS	F
Total	1	34		
Correlation	.599	1	.599	49.31
Residual	.401	33	.012	

The F calculated from this table was also highly significant on the 1% level.

Thus, both the regression coefficients and the linear correlation coefficient were found to be significant in a statistical sense. Examination of the scatter diagram (see Fig. 9) showed that the regression line was practically equidistant from the abscissa,  $X_1$ , and the ordinate,  $X_2$ , and passed quite close to the origin. These above results of the initial rainfall correlation study clearly indicated that the equation for the estimate of rainfall from the monthly frequency of highly reflective cloudiness,  $X_2' = 68.9 + 40.9X_1$ , could realistically be used in both

an areal and quantitative sense.

CHAPTER IV  
EL-NINO DATA COLLECTION

The expansion of the data set to include the period prior to and following the El-Nino of 1972-1973 entailed three steps; the training of new personnel, the quality control of the input and output data, and the development of a program to produce more usable data formats.

To facilitate the data assembly, three undergraduate students were trained to extract the highly reflective cloud masses from the satellite mosaics. First, the students were shown pictures of the various types of clouds and cloud masses found over the tropical oceans. Then they were shown examples of the appearance of these cloud masses on the satellite mosaics. Overdeveloped and underdeveloped mosaics were used to show the students the variations in brightness that were typical of the highly reflective cloud masses. The probable climatological variations of these cloud masses were discussed, and the inaccuracy of satellite gridding pointed out through the use of examples on the NOAA mosaics. These examples included five degree misplots of data, passes that were plotted out of sequence, passes compiled backward, and passes listed twice in succession. All of these gridding errors can usually be recognized by repetitious data or by

abrupt shifts of the near equatorial maximum cloudiness zone.

The students were then shown how to use individual shapes and combinations of shapes to correctly fit the clouds, how to locate the center grid point of the shape, and how to code the seven digit number that identifies the orientation, the size, and the position of the cloud masses. Data for ten day periods in the month of August 1972 was then individually compiled by each student. These ten day totals were then compared to the ten day totals compiled by the author during the pilot study. When no significant areal or quantitative differences were observed the student was then utilized to compile the El-Niño data collection.

The computer program that transformed the seven digit number into an area incrementation in the two dimensional array rejected this number if its fields were not within the range of the variables they represented. When this occurred, the program printed this number in its incorrect form. Thus, most coding and keypunching errors were easily corrected. The output data was then reviewed and any variations from the expected climatology were verified by examination of the NOAA mosaics.

A computer program was then developed to produce unanalyzed charts showing the monthly totals of the number of days of highly reflective cloud cover from 20°N to 20°S

and from 125°E to 80°W in the Northern Hemisphere and 150°E to 80°W in the Southern Hemisphere. These charts were then hand-analyzed and the areas of cover in three day increments of highly reflective cloud cover were outlined (see Fig. 10). These analyzed charts in a one degree grid were completed for the period between May 1971 and January 1974. This same program was then modified to produce an unanalyzed chart that maps the difference between two chosen time periods in units of the number of days of highly reflective cloud cover. Charts were then produced that subtracted every month not included in the period of the El-Niño phenomenon from every month included in the time period of the phenomenon, in other words, the highly reflective monthly cloud totals for the individual months from May 1971 to April 1972 and the totals for the individual months from May 1973 to January 1974 were subtracted from the totals for the individual months from May 1972 to April 1973. These charts were then hand-analyzed and the areas of cloud cover in three day increments were outlined. The positive areas represented the extent of the geographic regions where highly reflective cloudiness was greater in the month included in the El-Niño time period and the negative areas showed where the cover was greater during the pre or post El-Niño period (see Fig. 11).

An integer number that was the sum of all the grid



points in the array was also printed on the charts. This number was useful as it represented the total number of days of highly reflective cloud found in the one degree grid array during the time period studied. This number divided by the total number of grid points included in the array times the number of days the study encompassed gave the percent of the area that was covered by highly reflective clouds during the selected period. A sum was calculated for latitude strips and a cross section was plotted (see Fig. 12). This number divided by the total number of grid points included in the latitude strip times the number of days the study encompassed, gave the percent of the latitude strip that was covered by highly reflective clouds. Also, this number, the sum of all the grid points in a latitude strip, divided by the previously calculated integer, the sum of all the grid points in the array, gave the percent of the highly reflective clouds that the latitude strip contributed to the total. A sum was calculated and the cross section plotted for latitude strips in forty degree increments (see Fig. 13), and the above mentioned percentages obtained for these smaller grid partitions by using the same procedures. Cross sections showing the average monthly number of days of highly reflective cloud cover for latitude strips were also printed in the data output formats. These included coverage in latitude strips for the total Pacific Ocean

area (see Fig. 14), for forty degree and twenty degree increments of the Pacific Ocean area (see Fig. 15 and Fig. 16), and for selected five degree cross sections (see Fig. 17). These cross sections were plotted in two scales, the one shown in Figs. 15-17, and the smaller scale found in Figs. 18-20. The scale used in Figs. 15-17 was useful in an examination of the gradient of the average number of days of highly reflective cloud cover. The scale used in Figs. 18-20 lent itself to the examination of major features in the cloud field. Plots that showed the average number of days of highly reflective cloud cover for longitude strips, and number of days of highly reflective cloud coverage for selected longitudes are found in Fig. 21 and Fig. 22.

An integer number that represented the sum of all the grid points was also printed on those charts that mapped the difference between two time periods. This integer indicated which time period had the greatest number of days of highly reflective cloud. A sum for the difference in the number of days of cover for latitude strips was calculated and plotted for the total Pacific Ocean area and for forty degree increments of this area (see Fig. 23 and Fig. 24). These were used to ascertain the latitudes in which major changes in the mapped field occurred. Individual plots that showed the difference in the average cover for the total Pacific region and for

forty degree increments of the region were also included in the output (see Fig. 25).

In addition to the above mentioned data formats, the original seven digit number was processed on magnetic tape. This facilitated the compilation of yearly totals of highly reflective cloudiness. In fact, the computer program coupled with the magnetic tape can produce all the above mentioned data formats for any desired time period between May 1971 and January 1974.

CHAPTER V  
FINAL RAINFALL CORRELATION

A set of 820 monthly total rainfall observations between May 1971 and January 1974 were compiled to be used as the dependent variable, X2. These observations were limited to stations on coral islands that did not exceed an elevation of one hundred feet above sea level (see Appendix). The number of days of highly reflective cloud for the same month at the exact geographic position of the respective stations were listed as the independent variable, X1. The computer program that incorporated Eqs. (2.1) to (2.7) was then used to calculate these statistics and plot a scatter diagram for each month. These scatter diagrams showed that both the regression equations and the correlation coefficients had a normal distribution. No seasonal variations were apparent in either the regression equations or the correlation coefficients.

About twenty-five observations per month were used to construct these scatter diagrams. As more monthly totals of rainfall were being collected from stations throughout the Pacific Ocean region, it was decided that a more detailed study of the independence of this variable would be attempted when this data set was maximized. Thus,

the computer program that incorporated Eqs. (2.1) to (2.7) was used to plot a scatter diagram for the period between May 1971 and January 1974 (see Fig. 26).

As in Chapter III, analysis of variance tables for testing the significance of regression relationship and the correlation coefficient were constructed.

Table 3

Analysis of Variance Table for  
Testing the Significance of a Regression Relationship

Source	SS	dof	MS	F
Total	18543562.1	819	22641.7	
Slope of regression line	10405356.6	1	10405356.6	1051.81
Deviations from regression	8111679.1	818	9916.5	

Table 4

Analysis of Variance Table for  
Testing the Significance of the Correlation Coefficient

Source	SS1	dof	MS	F
Total	1	819		
Correlation	.563	1	.563	1052.33
Residual	.437	818	.00535	

The regression relationship,  $X_2' = 55.3 + 39.2X_1$ , was tested and the F shown in Table 1 found to be highly significant. The 1% limit for one and 818 degrees of

freedom (see Table 19 of Panofsky and Brier, 1968) was 6.67 compared to the observed F of 1051.81. The correlation coefficient, .75, was also highly significant on the 1% level.

Examination of the scatter diagram (see Fig. 26) showed that the regression line was practically equidistant from the abscissa and the ordinate and passed quite close to the origin. The regression relationship had reduced the scatter by about 35%. Thus, the quantitative estimates of rainfall had a moderately wide range of confidence. The vast majority of this scatter was probably caused by the fact that we used satellite information which only gave us the distribution of highly reflective cloud once a day. Rain could and did fall anytime, and there is no doubt that the instantaneous satellite pictures did not show many of the highly reflective cloud masses that existed during the twenty-four hour period. However, some of this scatter was probably caused by inaccuracies in rainfall measuring techniques, and thus, the author thought that the regression equation gave more accurate predictions than this statistic indicated.

Using the same set of rainfall observations as the dependent variable, X2, the average monthly cloud cover in oktas for the same time period was listed as the independent variable, X1. These values of X1 were obtained from Sadler's nine year study of mean satellite cloud

cover, which is an extension of his earlier study (Sadler, 1969). As nephanalysis averages have been utilized in the compilation of several more recent rainfall estimates (Barrett, 1970; Taylor, 1973), it was thought that this was a good opportunity to test this technique. Thus, the statistics, Eqs. (2.1) to (2.7), were calculated and the scatter diagram plotted (see Fig. 27). These statistics were used to construct analysis of variance tables.

Table 5

Analysis of Variance Table for  
Testing the Significance of a Regression Relationship

Source	SS	dof	MS	F
Total	18264618.8	650	28099.4	
Slope of regression line	5203768.8	1	5203768.8	258.4
Deviations from regression	13060817.7	649	20124.5	

Table 6

Analysis of Variance Table for  
Testing the Significance of the Correlation Coefficient

Source	SS1	dof	MS	F
Total	1	650		
Correlation	.285	1	.285	259.0
Residual	.715	649	.0011	

The regression relationship,  $X_2' = -347.3 + 139.2X_1$ , and

the correlation coefficient, .53, were both significant on the 1% level. However, examination of the scatter diagram shows that though the cloud cover in oktas may be used in a qualitative sense, quantitatively the equation should not be used to estimate rainfall.



CHAPTER VI  
CONCLUSION AND DISCUSSION

The regression relationship had been established. Within the limits of the statistical results, the regression equation could now be used to estimate the rainfall for the period between May 1971 and January 1974. Though the analyzed charts and cross sections were in units of the number of days of highly reflective cloud cover, rainfall estimates were easily calculated through the use of the regression equation. For example, in the month of May 1972, the latitude strip at six degrees north averaged twelve days of highly reflective cloud cover (see Fig. 14). This equated to a rainfall average of 526 millimeters.

The rainfall for selected periods between May 1971 and January 1974 was estimated. A major question remained. How realistic were these estimates? Early rainfall cross sections by Wuest (1936) and Meinardus (1934) were shown in Jacobs (1951). Jacobs (1951) also produced his own estimates. Schott (1935) produced a chart that showed annual precipitation over the Pacific Ocean. Meinardus' and Schott's estimates were judged to be an accurate areal representation. However, the values of the isohyets were thought to be overestimated (Haurwitz and Austin, 1944; Jacobs, 1951). As Wuest based his open ocean rainfall

estimates on an analysis of the fields of ocean surface salinity and evaporation, they were generally accepted as being quantitatively more accurate (Jacobs, 1951; Riehl, 1954). In a more recent study, Taylor (1973) compiled a collection of island station monthly rainfall totals and used satellite cloud cover that was compiled by Sadler (1969) as a guide in plotting both the gradient and values of the isohyets. All of these above estimates (except Schott's) and the annual rainfall estimate calculated from the highly reflective cloud (HRC) were plotted on a cross section (see Fig. 28).

Examination of Fig. 28 showed that in the region south of the equatorial dry zone the HRC annual rainfall estimate agreed most closely with Wuest's estimate. In the area of this dry zone the slope of the curve agreed with Taylor's and the HRC estimate was markedly lower than any other estimate. In the area of maximum rainfall,  $5^{\circ}\text{N}$  to  $10^{\circ}\text{N}$ , the closest agreement was found with Meinardus and the slope of the curve again agreed with Taylor's. North of the maximum rainfall zone, the slope agreed most closely with that of Taylor's and the final quantitative value approached that of Wuest's.

The examination of the rainfall estimate compiled by Taylor and the HRC estimate showed two marked differences. The first, that Taylor's estimate of annual precipitation, excluding the area from  $10^{\circ}\text{N}$  to  $20^{\circ}\text{N}$ , was approximately

80% higher. The second, that Taylor found distinct rainfall maxima at  $10^{\circ}\text{S}$  and  $6^{\circ}\text{N}$ .

As Taylor used Sadler's cloud cover in the compilation of his estimate, Sadler's nine-year annual mean was examined and the maximum cloud cover for the Pacific Ocean region was found to be 4.7 oktas at  $6^{\circ}\text{N}$ . Using the regression equation derived in Chapter V, this equated to 307 centimeters of rainfall.

Since the thirty-three month period the HRC study encompassed might not have been truly representative of a long term annual precipitation estimate, a closer study of the yearly rainfall totals seemed in order. Thus, three periods were examined separately and a cross section plotted that showed the annual precipitation for May 1971 to April 1972, May 1972 to April 1973, and May 1973 to January 1974 (see Fig. 29). The period May 1973 to January 1974 was extrapolated to estimate the annual precipitation for the period May 1973 to April 1974. The NOAA satellite mosaics supported the extrapolation as the highly reflective cloud cover during February, March, and April 1974 was typical of the nine month period that preceded it.

Rainfall observations for the first period, May 1971 to April 1972, were examined (Taylor, 1973). They indicated that this period was one of relatively normal activity. Sadler's cloud analysis for this period was examined and no significant variations from the nine-year mean were

observed.

The period from May 1972 to April 1973 was then examined. Though this period had significantly different rainfall patterns, the total rainfall was the same as in the previous period. Although a detailed discussion of the rainfall patterns in this period is not within the scope of this paper, two major differences between the May 1971 to April 1972 and the May 1972 to April 1973 rainfall patterns warrant a brief discussion.

The first major difference occurred in the second period, May 1972 to April 1973. Much lower rainfall estimates were found between  $20^{\circ}\text{N}$  and  $8^{\circ}\text{N}$ . During this second period the near equatorial maximum rainfall zone did not migrate north as it did in the first period, but stayed near  $5^{\circ}\text{N}$  to  $6^{\circ}\text{N}$ . This phenomenon coupled with a marked lack of midlatitude activity south of  $20^{\circ}\text{N}$  produced the lower rainfall estimates between  $20^{\circ}\text{N}$  and  $8^{\circ}\text{N}$  for the second period.

The second major difference was the higher rainfall estimates during the second period from  $6^{\circ}\text{N}$  to  $10^{\circ}\text{S}$ . An area of relatively high precipitation encroached from the west into the near equatorial dry zone to approximately  $150^{\circ}\text{W}$ . This coupled with the relative stability of the near equatorial maximum rainfall zone during the second period produced higher estimates in the equatorial zone.

Further examination of Fig. 29 showed that though both

twelve month periods averaged approximately 133 centimeters of rainfall in the Pacific Ocean region, the nine month period, May 1973 to January 1974, extrapolated to a twelve month average of only 74 centimeters for the Pacific Ocean region. Thus, the third period, the twelve month extrapolation that represented the period between May 1973 and April 1974, was clearly the most anomalous. It was obviously a period of drought in the Pacific Ocean region. Though a period of drought will occasionally occur in this region, this does not normally happen in one out of every three years.

Thus, one can conclude that the annual precipitation calculated from this thirty-three month period was at least 20% below what a truly long term study might yield. Increasing the author's rainfall estimate shown in Fig. 28 by this factor did give a better agreement with Taylor's estimate in the area between  $20^{\circ}\text{N}$  and  $12^{\circ}\text{N}$ . It did not account for the 80% difference between these two rainfall estimates south of  $12^{\circ}\text{N}$ .

Two large areas of maximum rainfall on Taylor's annual precipitation chart were examined. One was located near  $5^{\circ}\text{N}$  and  $170^{\circ}\text{E}$ , the other near  $10^{\circ}\text{S}$  and  $170^{\circ}\text{E}$ . Both maxima showed values approximately 100 centimeters higher than the author's study. The maximum at  $10^{\circ}\text{S}$  and  $170^{\circ}\text{E}$  was based on two stations; Sola, Vanualava in the New Hebrides and Vanikoro on Santa Cruz. Similarly the maximum near  $5^{\circ}\text{N}$

and  $170^{\circ}\text{E}$  was based on one station, Kusaie in the Caroline Islands. All three of these islands are volcanic. The highest point on Vanualava is Mount Suretamati at 913 meters. Further examination showed that the majority of the island stations Taylor used were volcanic. I question the use of these stations. They have orographic effects, and their rainfall measurements were not representative of open ocean precipitation.

I could not explain Taylor's sharp gradient within the maximum rainfall zone. The seasonal migration of this zone (Riehl, 1954; Taylor, 1973) was expected to produce a smaller gradient from about  $5^{\circ}\text{N}$  to  $9^{\circ}\text{N}$  (see Fig. 28).

As mentioned before, the study of Wuest, because of its balance of precipitation with an analysis of open ocean surface salinity and evaporation, was thought to be quantitatively accurate. Thus, I was encouraged by the general quantitative agreement in the area from  $5^{\circ}\text{S}$  to  $20^{\circ}\text{S}$  between the HRC estimate and Wuest's estimate. The quantitative disagreement between  $15^{\circ}\text{N}$  and  $5^{\circ}\text{S}$  was noted. However, both the larger values produced by Wuest in the equatorial dry zone and smaller values found in the area of maximum rainfall could be explained by the advection into these areas of waters of different salinity. Over most of the area from  $5^{\circ}\text{S}$  to  $20^{\circ}\text{S}$  in the Pacific Ocean, the currents are northwesterly. Since the rainfall in this area appeared to be relatively constant, the advection of water

of a different salinity would not drastically change the balance between ocean surface salinity, evaporation, and precipitation. However, the advection of water from the relatively higher rainfall area between  $5^{\circ}\text{S}$  and  $20^{\circ}\text{S}$  to the arid section of the Pacific Ocean between  $2^{\circ}\text{N}$  and  $5^{\circ}\text{S}$  would disturb this balance and support an overestimation of rainfall in the near equatorial dry zone. Similar reasoning could be used in the area from  $15^{\circ}\text{N}$  to  $3^{\circ}\text{N}$ . Water advected from an area of lower rainfall to higher rainfall by the southwesterly currents would support a lower precipitation total. Mixing of the ocean surface water with deeper water would probably aid the advective influences and smooth the field of salinity even more.

Of the rainfall estimates examined the only cross section not plotted was that of Schott (1935). Examination of his rainfall analysis showed that a cross section scaled from his data would probably have been quite similar to that of Meinardus'. Riehl (1954) stated his preference for Meinardus' charts solely on the grounds that Wuest's rainfall values in the area from  $3^{\circ}\text{N}$  to  $10^{\circ}\text{N}$  could not be reconciled with the higher amounts measured on many of the small atolls in the northern Pacific Ocean (see, for example, Taylor, 1973). The results of this study supported Riehl's observation. In this area of maximum rainfall from  $10^{\circ}\text{N}$  to  $3^{\circ}\text{N}$  the estimates of Schott and Meinardus were probably the most accurate.

As a final test the average annual precipitation in the area  $20^{\circ}\text{N}$  to  $15^{\circ}\text{N}$  and  $160^{\circ}\text{W}$  to  $140^{\circ}\text{W}$  was calculated. This is an area of very persistent trade winds. The annual precipitation in this region was 59 centimeters for the period between May 1971 and January 1974. This was quite close to other estimates of open ocean rainfall for the Hawaiian region (Stidd and Leopold, 1951; Blumenstock and Price, 1967).

The compiled magnetic tape and a computer program that includes the regression equation can now be used with some confidence to produce rainfall estimates in a one degree grid. These rainfall estimates have many meteorological and oceanographic applications. As heat energy is taken from the sea surface in the change from liquid to vapor and given to the atmosphere in the process of condensation, they can be used in areal and quantitative estimates of vertical heat transports over the open ocean. The large areas of rainfall maxima and minima can be indicative of zones of rising and sinking air associated with meridional and zonal circulations. The rainfall estimates can be correlated with certain oceanographic data sets, for instance, measurements of sea surface salinity or sea surface temperature. The estimates can also be used in conjunction with other meteorological variables, such as the wind field and evaporation estimates, to map areas of water vapor advection.



Thus, accurate long term estimates of tropical open ocean rainfall in the Pacific Ocean region were made available for May 1971 to January 1974. The time period these studies encompassed was not selected at random. It preceded, included, and immediately followed the El-Niño phenomenon of 1972-1973. Therefore, the major contribution of these rainfall estimates will be their usefulness in the study of the climatology and meteorology of this phenomenon.

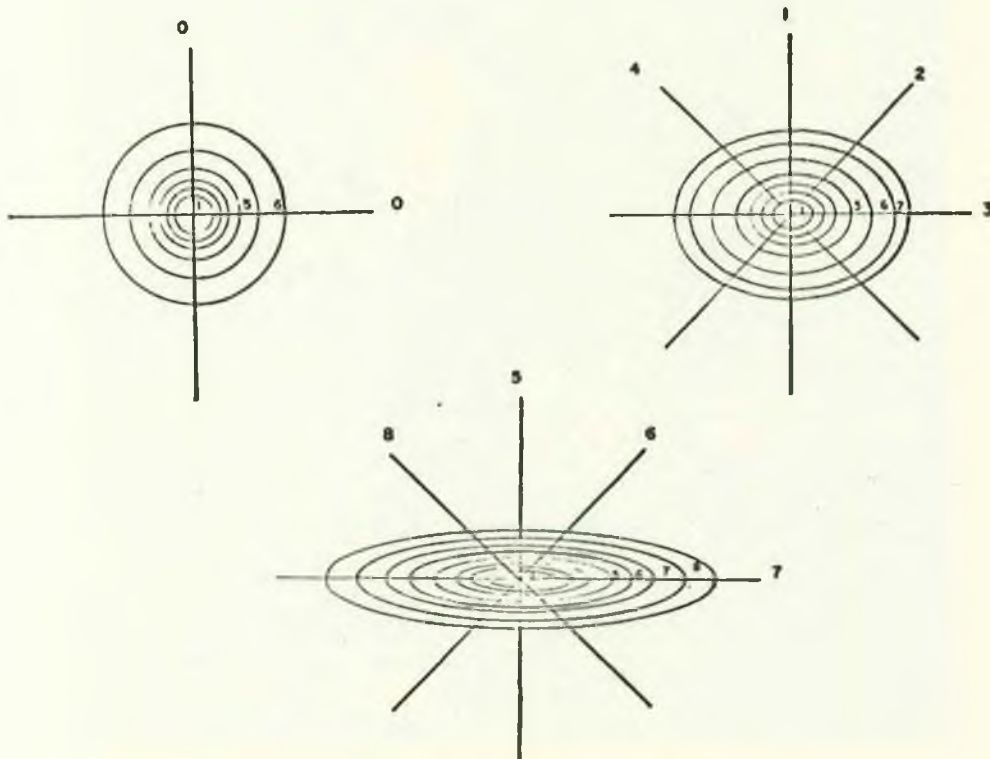


Fig. 1 Original draft of the six circles, seven wide ellipses, and eight narrow ellipses. Transparent overlays are made from this draft.

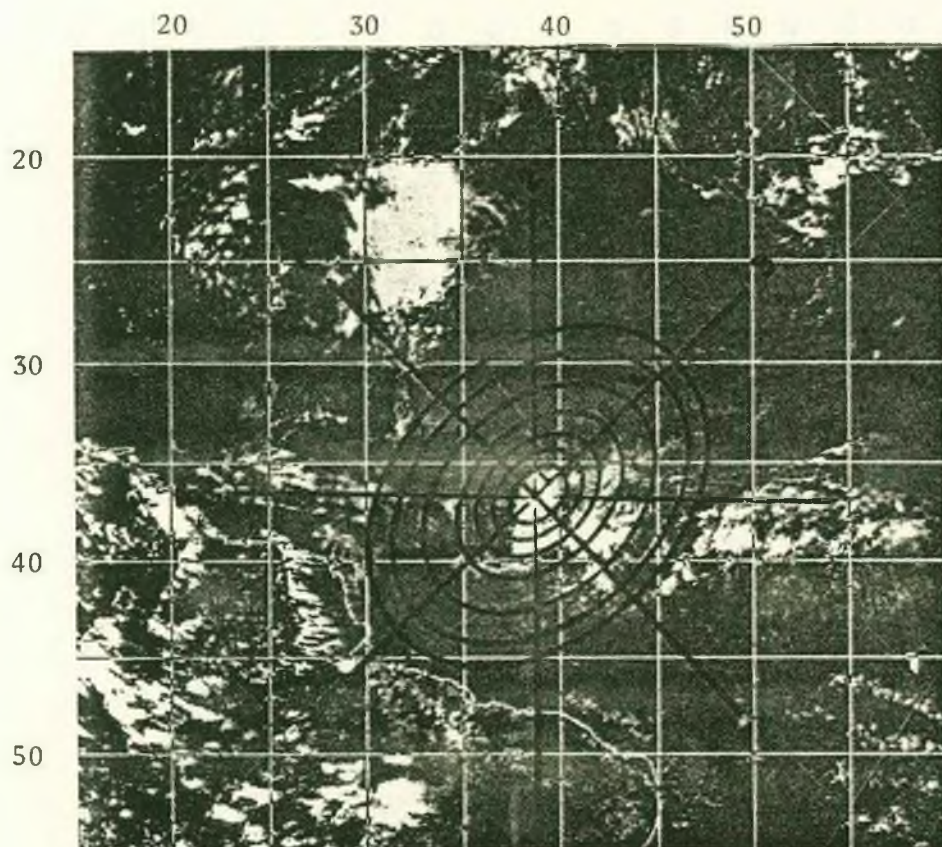


Fig. 2 Standard shape of orientation 2 and size 1 is correctly fitted to a highly reflective cloud mass on a NOAA digitized cloud mosaic. The center grid position is 37038.

0	0	0	0	0	0	0	0	0	0	C	0	0	0	0	C	0
0	0	0	0	1	1	1	0	0	0	C	0	0	C	0	C	0
0	0	0	1	1	1	1	1	C	0	C	0	0	0	0	0	0
0	0	1	1	1	1	1	1	1	0	C	0	0	0	0	C	0
0	0	1	1	1	1	1	1	1	0	0	0	0	0	0	0	0
0	0	1	1	1	1	1	1	1	0	C	0	0	0	0	C	0
0	0	0	1	1	1	1	1	0	0	C	0	0	0	0	0	0
0	0	0	0	1	1	1	0	0	0	2	2	2	0	0	0	0
0	0	0	0	0	0	0	0	0	2	2	2	2	2	0	0	0
0	0	0	0	0	0	0	0	2	2	2	2	2	2	2	C	0
0	0	0	0	0	0	0	0	2	2	2	2	2	2	2	0	0
0	0	0	0	0	0	0	0	2	2	2	2	2	2	0	0	0
0	0	0	0	0	0	0	0	0	0	2	2	2	C	0	0	0
0	C	0	0	0	0	0	0	0	0	C	0	0	0	C	0	0
0	0	0	0	0	0	0	0	0	0	C	0	0	0	0	0	0

Fig. 3 Shape 03 as it appears in a one degree grid mapping one and two days of highly reflective cloud cover.

```

0 0 0 0 0 0 0 0 0 0 0 0 0 0 0 0
0 0 0 0 0 0 0 1 1 1 0 0 0 0 0 0
0 0 0 0 0 0 0 1 1 1 0 0 0 0 0 0
0 0 0 1 1 1 0 1 1 1 0 1 1 1 0 0
0 0 0 1 1 1 1 1 1 1 1 1 1 1 0 0
0 0 0 1 1 1 1 1 1 1 1 1 1 1 0 0
0 0 0 1 1 1 1 1 1 1 1 1 1 1 0 0
0 1 1 1 1 1 1 1 1 1 1 1 1 1 1 0
0 1 1 1 1 1 1 1 1 1 1 1 1 1 1 0
0 1 1 1 1 1 1 1 1 1 1 1 1 1 1 0
0 0 0 1 1 1 1 1 1 1 1 1 1 1 0 0
0 0 0 1 1 1 1 1 1 1 1 1 1 1 0 0
0 0 0 1 1 1 0 1 1 1 0 1 1 1 0 0
0 0 0 0 0 0 0 1 1 1 0 0 0 0 0 0
0 0 0 0 0 0 0 0 0 0 0 0 0 0 0 0

```

Fig. 4 Shapes 54 to 84 mapped at the same grid center point and limited to a one unit per point per day incrementation.

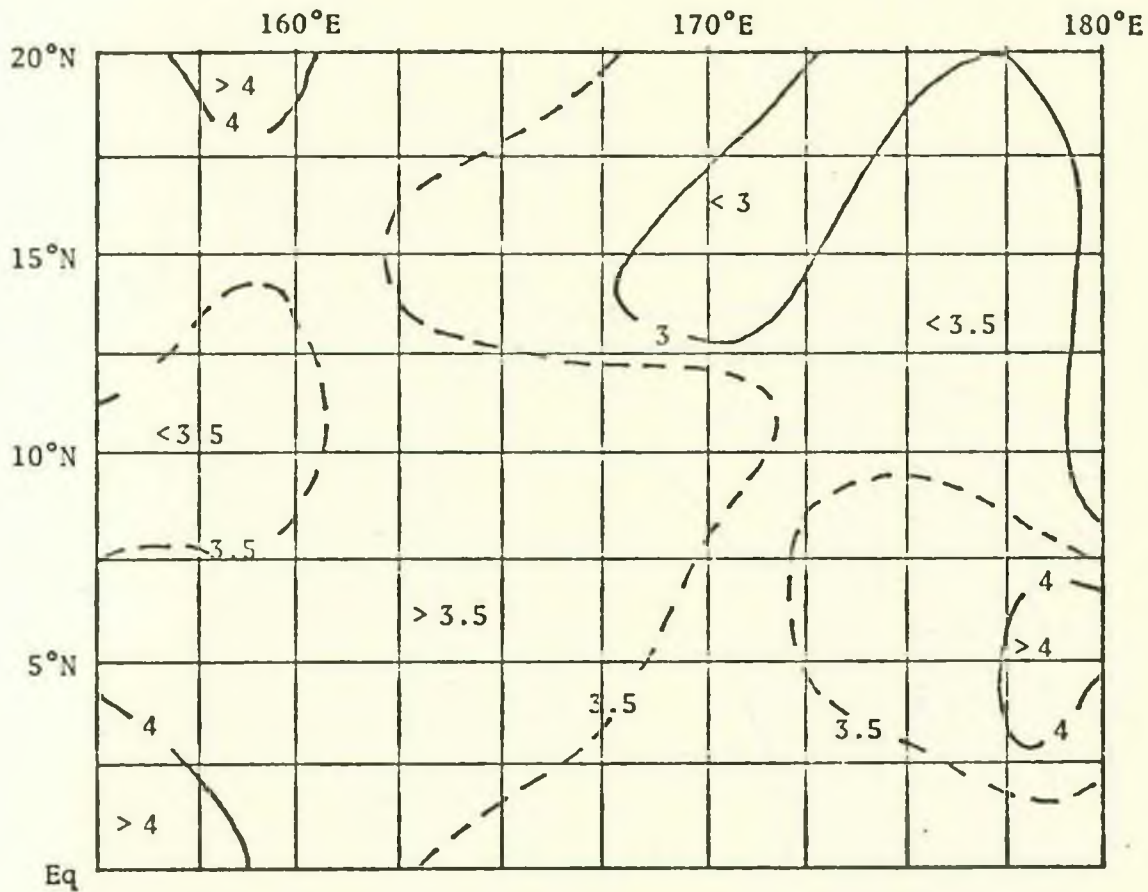


Fig. 5 Average cloud cover in oktas for the area 20°N to the equator and from 155°E to the date line for the period August 11, 1972 to August 20, 1972. This two and one half degree grid shows the same area and time period as Fig. 7.

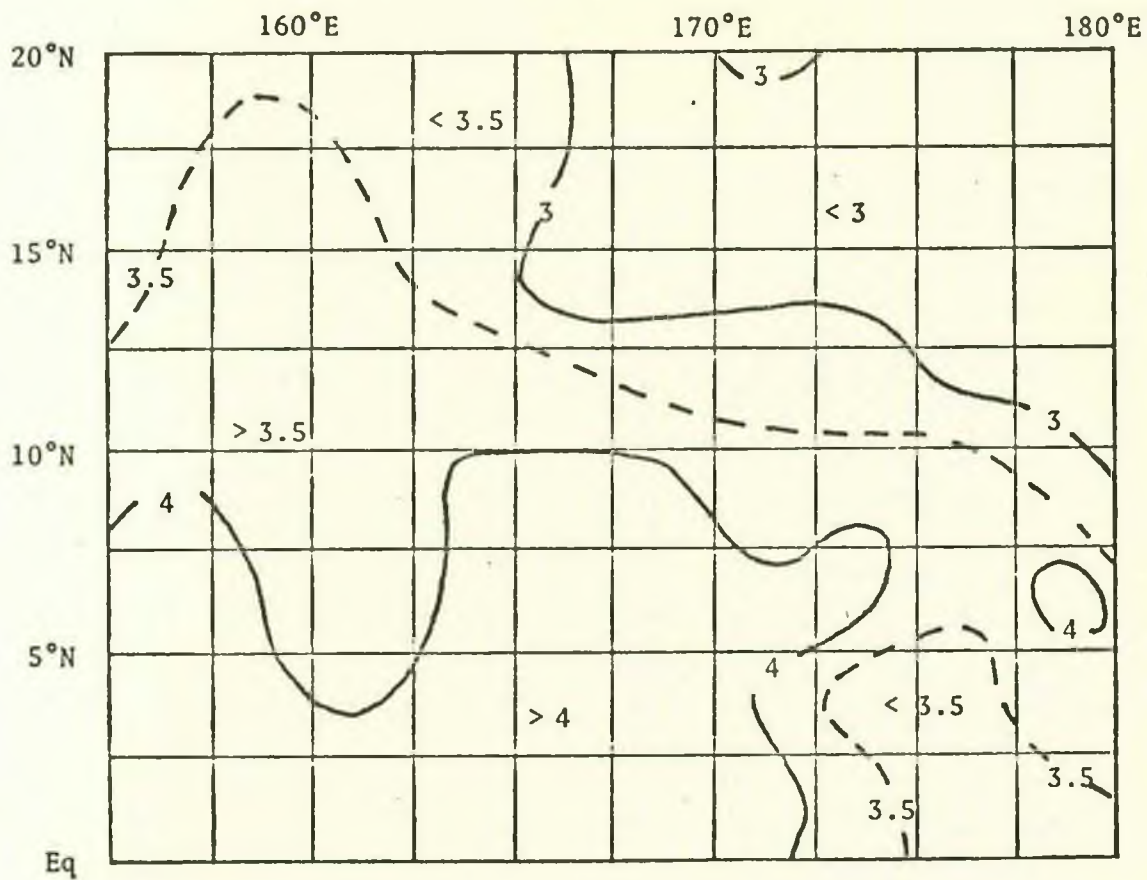


Fig. 6 Same as Fig. 5 except for the month of August 1972, and for comparison with Fig. 8.

## NUMBER OF DAYS COVERED BETWEEN 81172 AND 82072 (B)

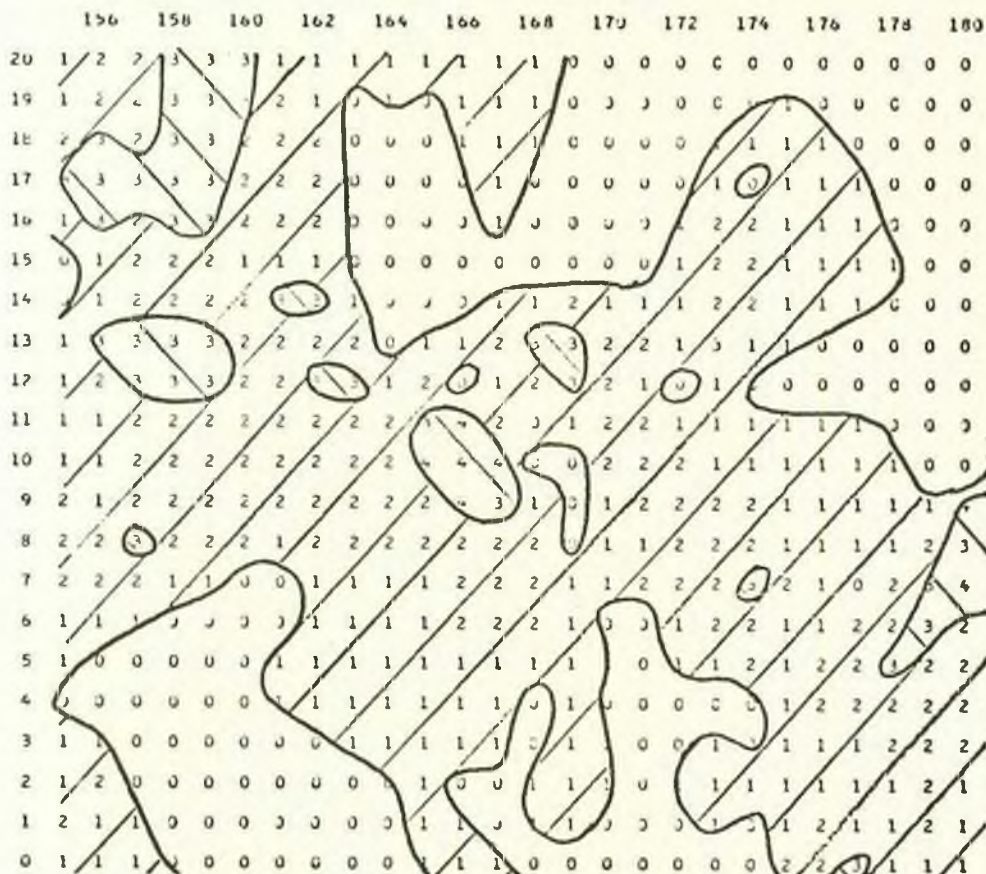


Fig. 7 Part of the hand-analyzed computer printout that maps the area from 20°N to 20°S and from 155°E to 80°W in a one degree grid. Areas of coverage are in two day increments of highly reflective cloud cover for the ten day period between August 11, 1972, and August 20, 1972. The area shown here is from 20°N to the equator and from 155°E to the date line.



## NUMBER OF DAYS COVERED BETWEEN 80172 AND 83172 (B)

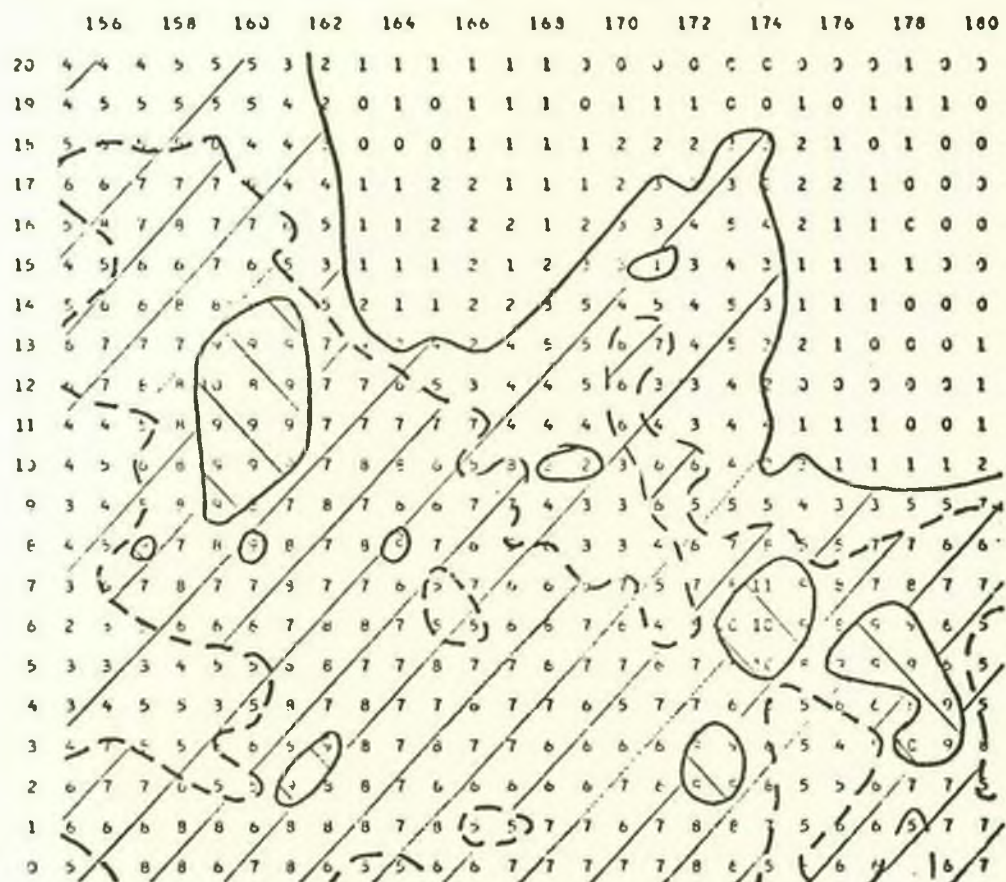
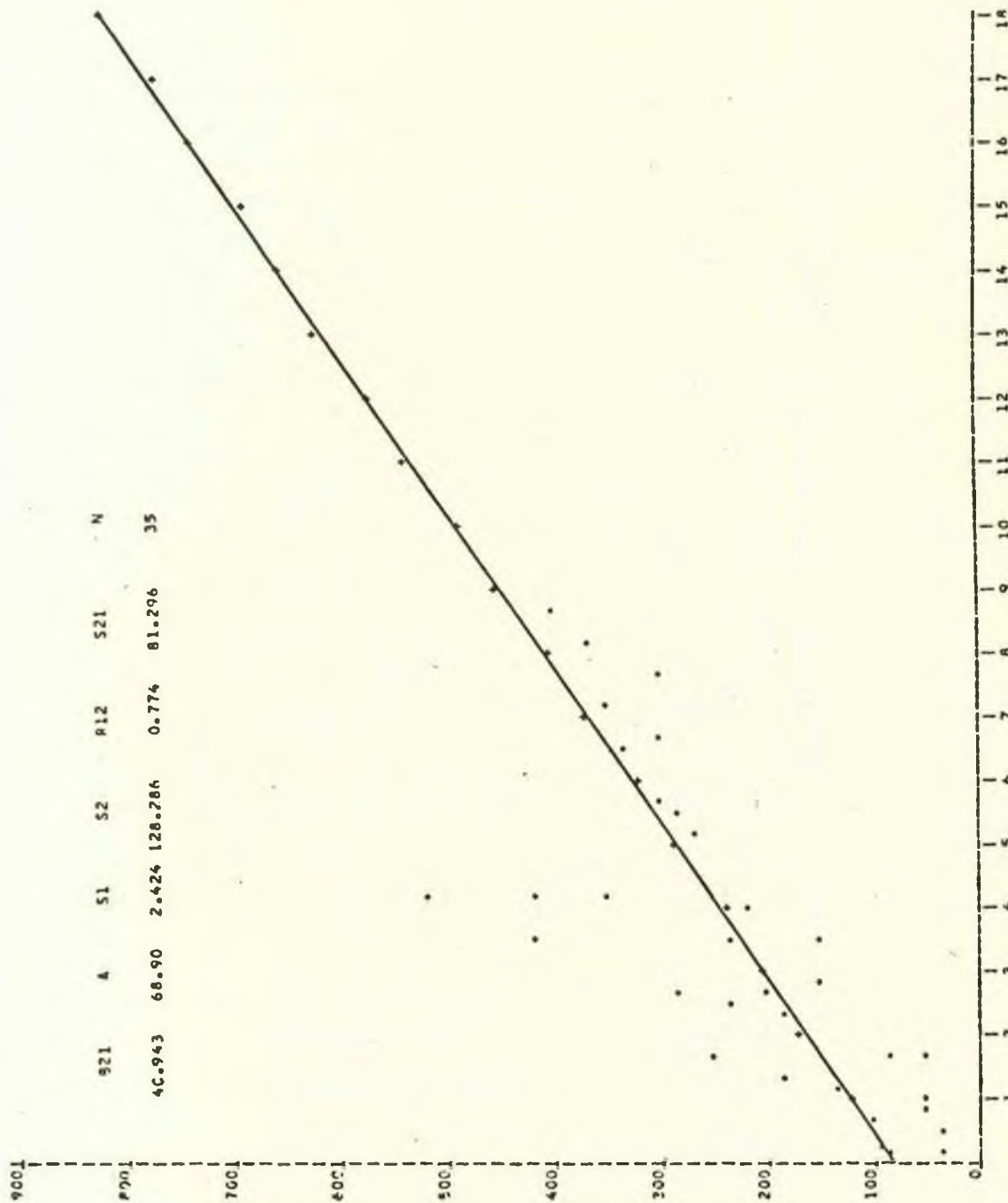


Fig. 8 Same as Fig. 7 except areas of coverage are in three day increments of highly reflective cloud cover for the month of August 1972.

Fig. 9 Statistics and scatter diagram derived from equations (2.1) to (2.7) for the month of August 1972. The vertical axis is in units of millimeters of rainfall. The horizontal axis is in units of the number of days of highly reflective cloud cover. The straight line is the least squares best fit.



## THE NUMBER OF DAYS OF HIGHLY REFLECTIVE CLOUD COVER DURING 8/72

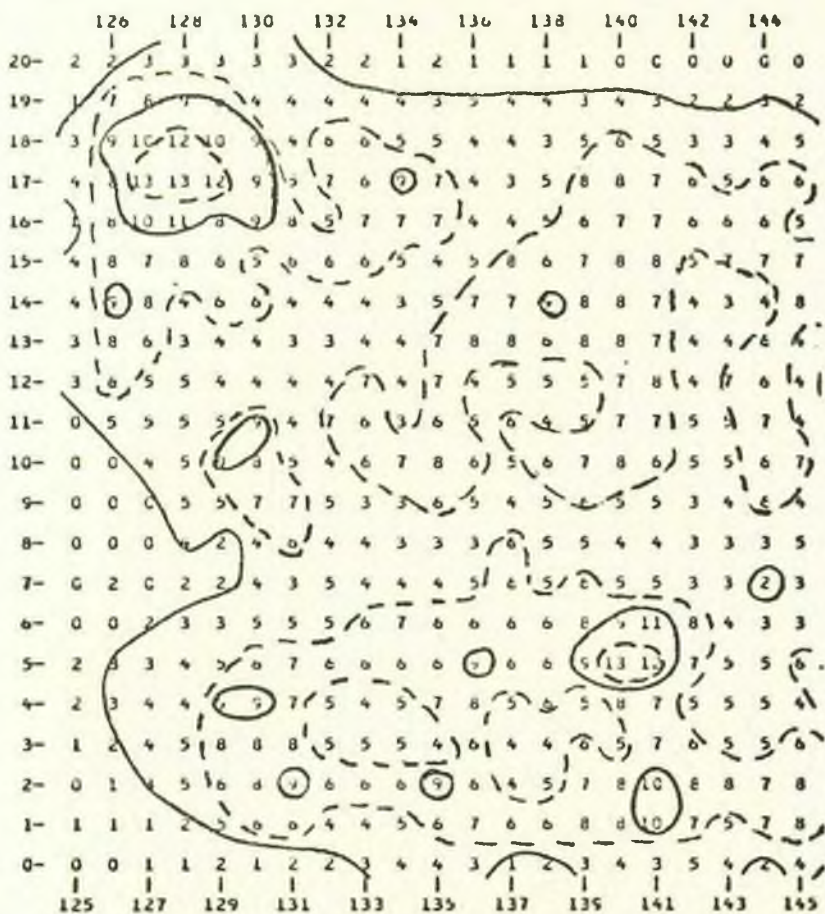
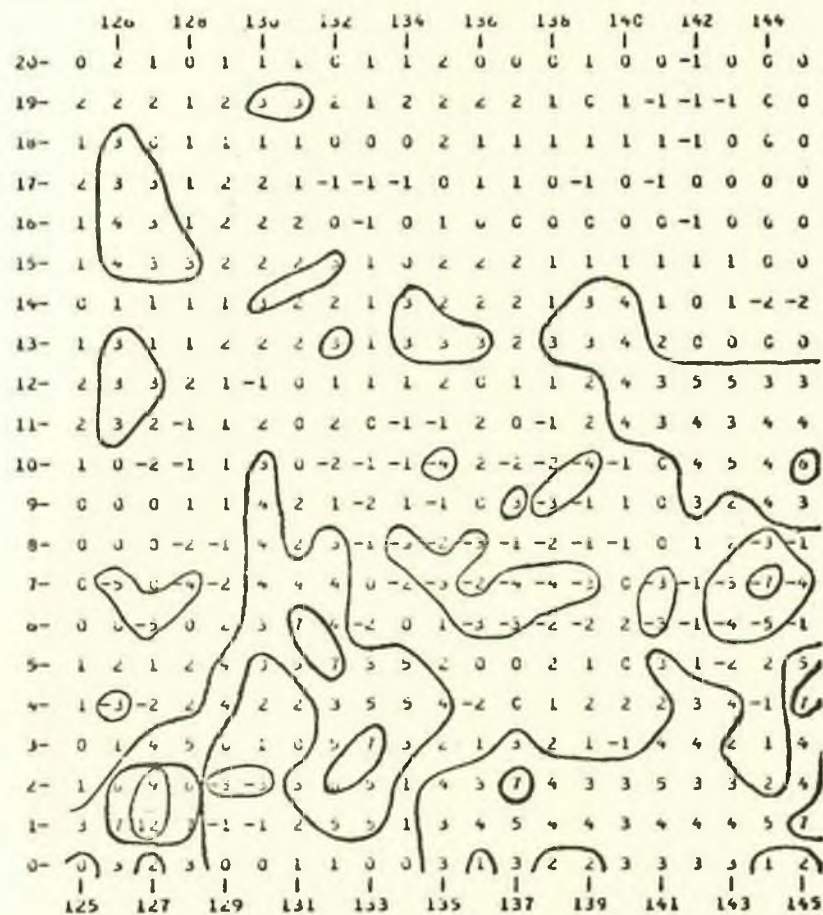


Fig. 10 Part of the hand-analyzed computer printout that maps the area from 20°N to 20°S and from 125°E to 80°W in the Northern Hemisphere and 150°E to 80°W in the Southern Hemisphere. Areas of coverage are in three day increments of highly reflective cloud cover for the month of August 1972.

## THE NUMBER OF DAYS OF HIGHLY REFLECTIVE CLOUD COVER DURING 5/72



MINUS THE NUMBER OF DAYS COVERED DURING 5/73

Fig. 11 Same as for Fig. 10 except the positive areas show where the coverage was greater in May 1972, the negative areas where it was greater in May 1973.

Fig. 12 Cross section,  $20^{\circ}\text{N}$  to  $20^{\circ}\text{S}$ , plotting the sum of the total number of days of highly reflective cloud cover for the month of August 1972 from  $125^{\circ}\text{E}$  to  $80^{\circ}\text{W}$  in the Northern Hemisphere and  $150^{\circ}\text{E}$  to  $80^{\circ}\text{W}$  in the Southern Hemisphere. The lower right-hand integer number (14474) is the sum of all the grid points in the area.

MONTH 8/72

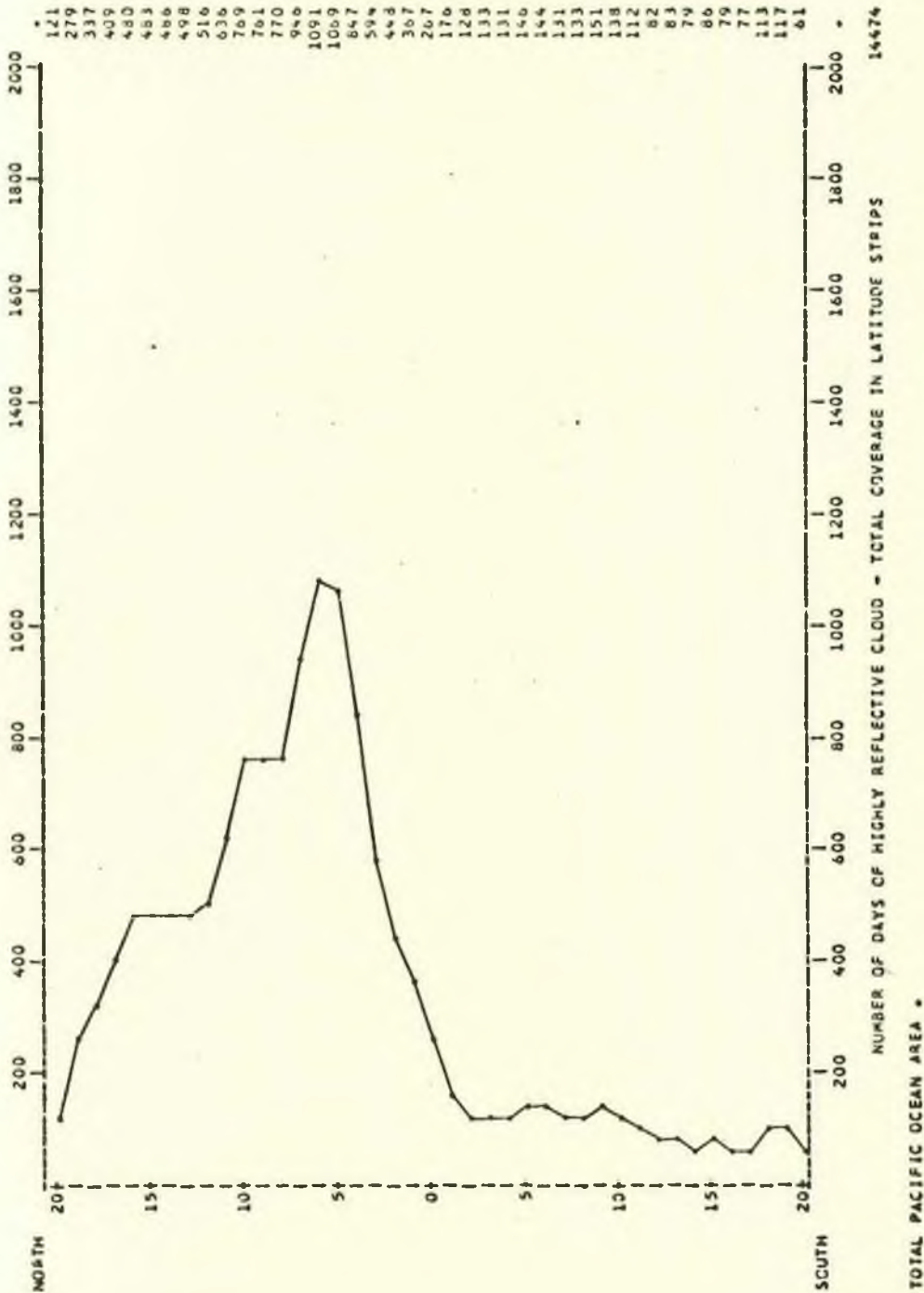
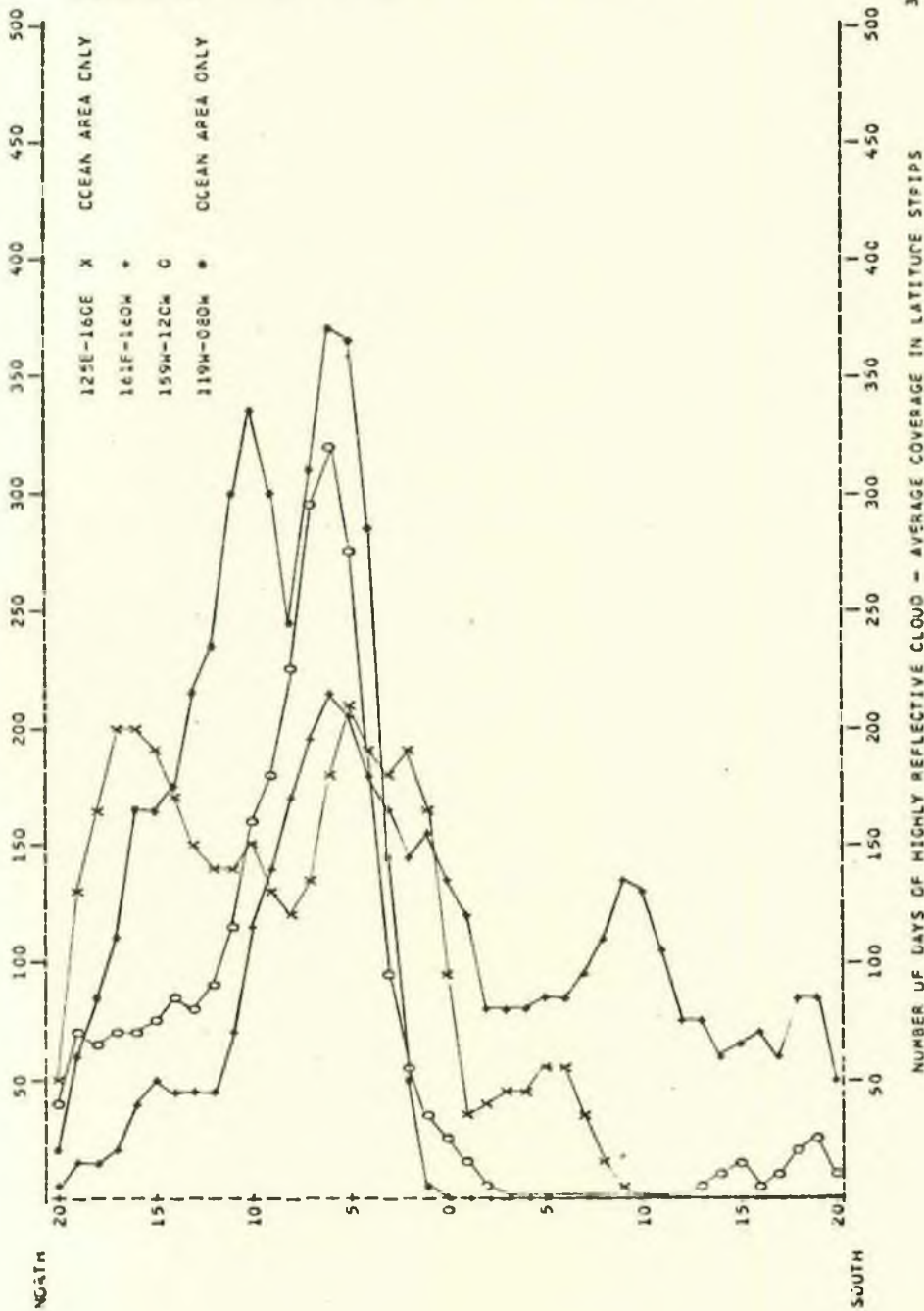


Fig. 13 Same as for Fig. 12 except the cross section is now plotted for forty degree increments of the Pacific Ocean region.



MONTH 8/72



x	50	7	42	22
	130	19	70	60
	165	19	66	67
	202	23	70	114
	200	40	71	169
	191	51	76	165
	172	49	89	176
	154	47	82	215
	140	48	93	235
	144	74	116	302
	152	116	162	339
	131	144	182	304
	123	172	227	248
	139	198	297	312
	181	219	320	371
	213	209	279	368
	191	180	190	286
	182	166	99	147
	193	140	53	54
	167	155	38	7
	96	139	29	3
	36	121	18	1
	40	81	7	0
	46	84	3	0
	47	82	2	0
	57	85	4	0
	56	87	1	0
	36	95	0	0
	17	114	2	0
	8	138	5	0
	4	130	4	0
	3	106	3	0
	3	75	4	0
	1	75	7	0
	2	63	14	0
	0	68	16	0
	0	70	9	0
	0	63	12	2
	0	88	22	3
	0	88	27	2
	0	50	11	0

3672 3984 2826 3982

NUMBER OF DAYS OF HIGHLY REFLECTIVE CLOUD - AVERAGE COVERAGE IN LATITUDE STRIPS

Fig. 14 Cross section,  $20^{\circ}\text{N}$  to  $20^{\circ}\text{S}$ , plotting the average number of days of highly reflective cloud cover for the month of May 1972 from  $125^{\circ}\text{E}$  to  $80^{\circ}\text{W}$  in the Northern Hemisphere and from  $150^{\circ}\text{E}$  to  $80^{\circ}\text{W}$  in the Southern Hemisphere.

MONTH 5/72



NUMBER OF DAYS OF HIGHLY REFLECTIVE CLOUD - AVERAGE COVERAGE IN LATITUDE STRIPS

TOTAL PACIFIC OCEAN AREA \*

Fig. 15 Same as Fig. 14 except the area is from  
161°E to 160°W.

MONTH 5/72



NUMBER OF DAYS OF HIGHLY REFLECTIVE CLOUD - AVERAGE COVERAGE IN LATITUDE STRIPS

101E-160M

Fig. 16 Same as Fig. 14 except the area is from  
139°W to 120°W.

MONTH 5/72



Fig. 17 Same as Fig. 14 except the area is from  
119°W to 115°W.



MCNTH 5/72

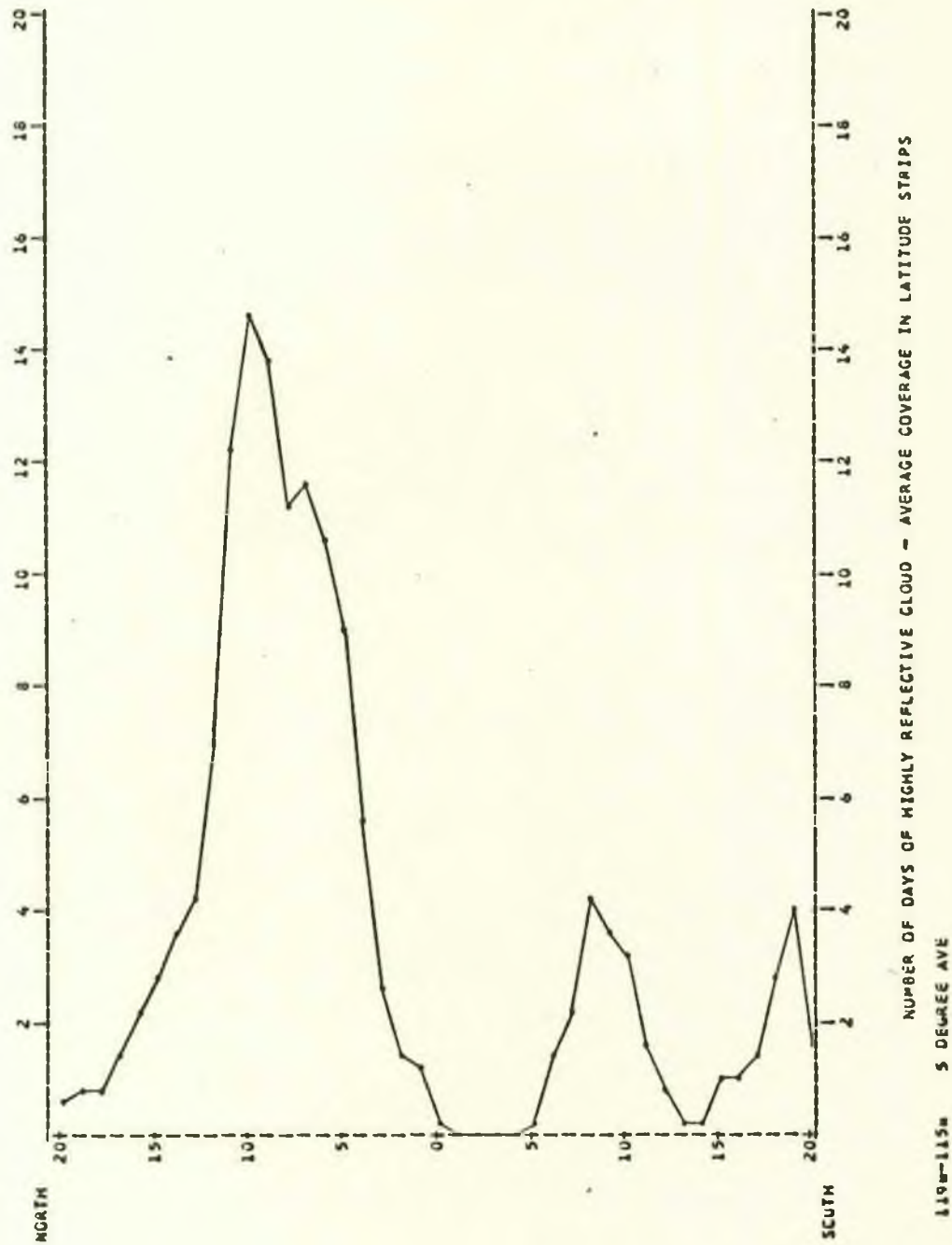
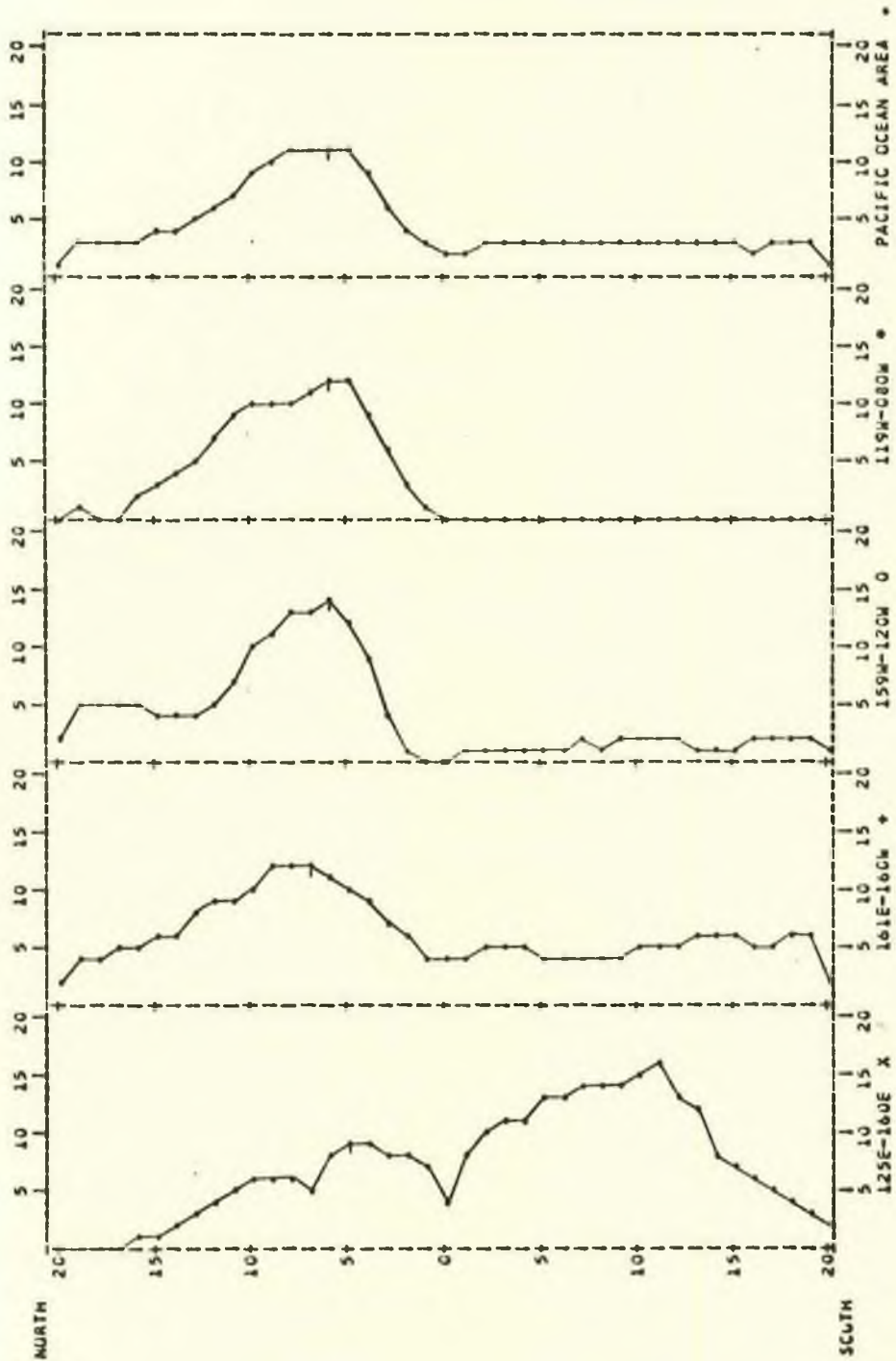


Fig. 18 Cross sections, 20°N to 20°S, plotting the average number of days of highly reflective cloud cover for forty degree increments and for the area of the Pacific Ocean.

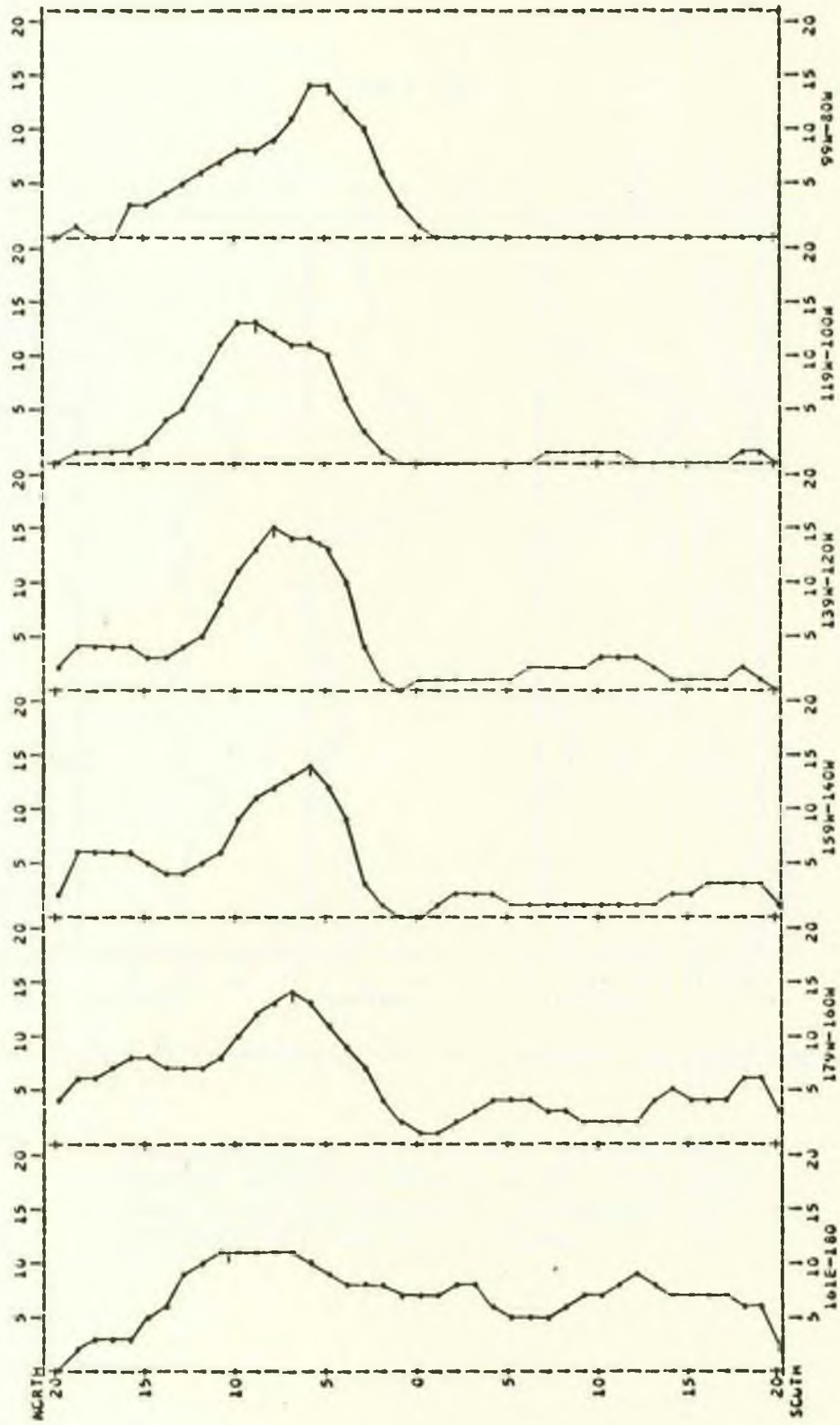
MONTH 5/72



NUMBER OF DAYS OF HIGHLY REFLECTIVE CLOUD - AVERAGE COVERAGE IN LATITUDE STRIPS

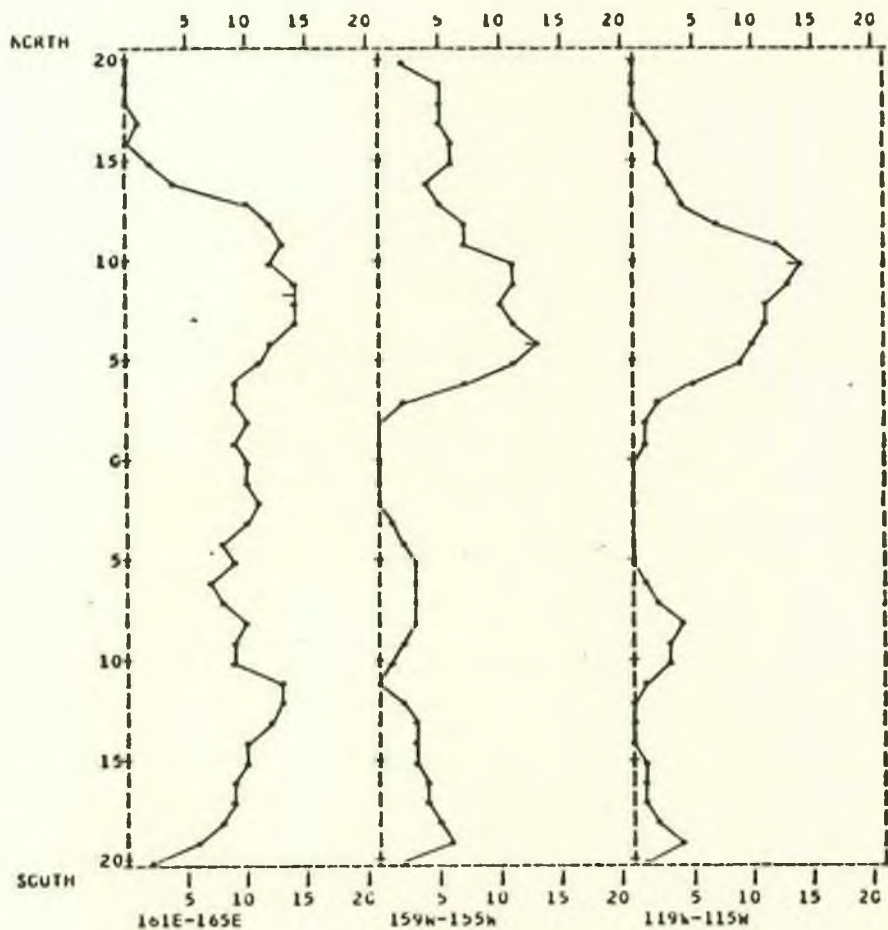
Fig. 19 Cross sections, 20°N to 20°S, plotting the average number of days of highly reflective cloud cover for twenty degree increments of the Pacific Ocean.

MONTH 5/72



NUMBER OF DAYS OF HIGHLY REFLECTIVE CLOUD - AVERAGE COVERAGE IN LATITUDE STRIPS

MUNTH 5/72



NUMBER OF DAYS OF HIGHLY REFLECTIVE CLOUD - AVERAGE COVERAGE IN LATITUDE STRIPS

Fig. 20 Cross sections,  $20^{\circ}\text{N}$  to  $20^{\circ}\text{S}$ , plotting the average number of days of highly reflective cloud cover for selected five degree increments of the Pacific Ocean.

Fig. 21 Average number of days of highly reflective cloud cover between  $20^{\circ}\text{N}$  and  $5^{\circ}\text{N}$ ,  $5^{\circ}\text{N}$  and  $5^{\circ}\text{S}$ ,  $5^{\circ}\text{S}$  and  $20^{\circ}\text{S}$ ,  $20^{\circ}\text{N}$  and  $20^{\circ}\text{S}$  listed and plotted from  $125^{\circ}\text{E}$  to  $170^{\circ}\text{E}$  or  $150^{\circ}\text{E}$  to  $170^{\circ}\text{E}$ . The full scale plot, of which this figure is a part, extends to  $80^{\circ}\text{W}$ .

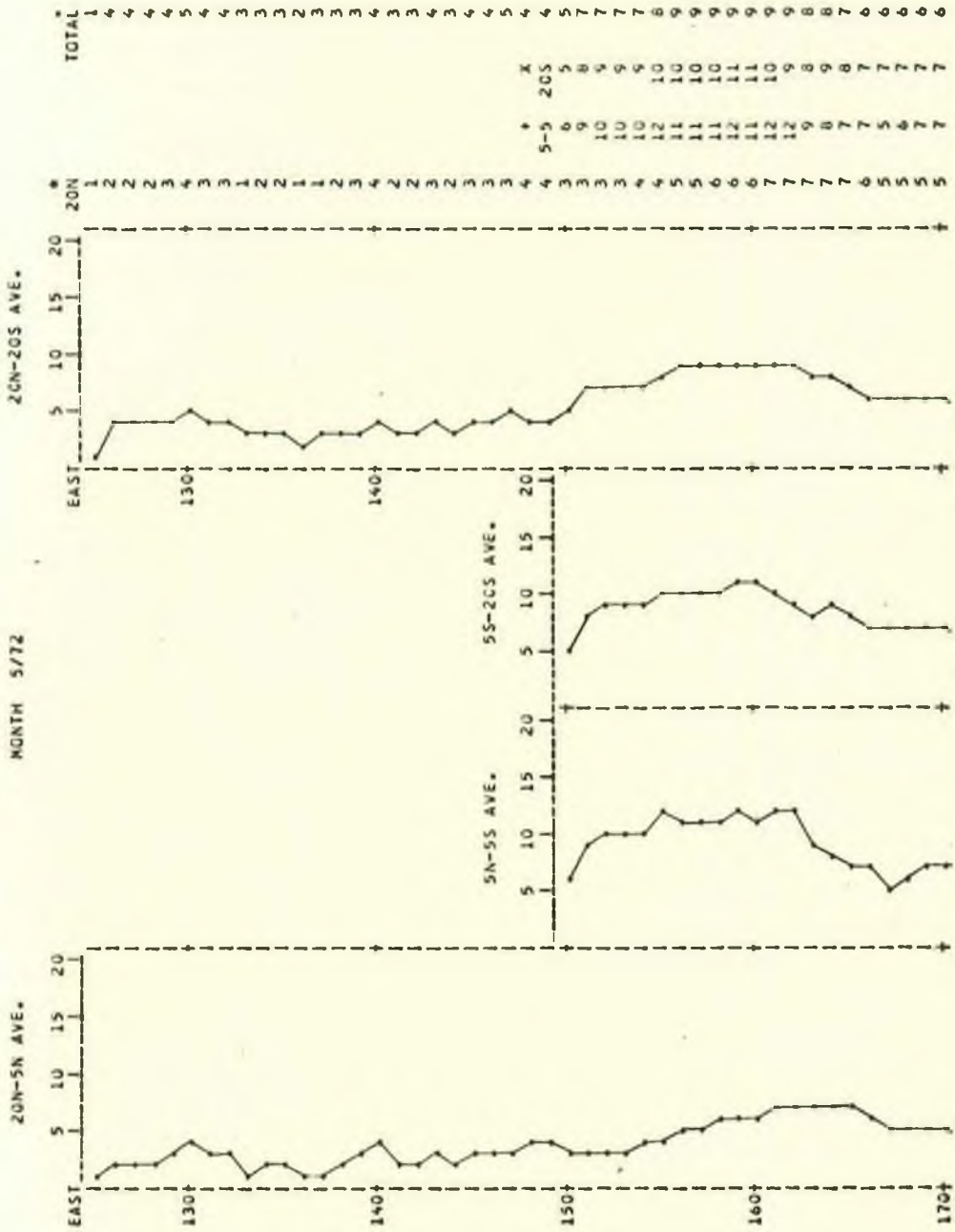




Fig. 22 Number of days of highly reflective cloud cover at  $10^{\circ}\text{S}$ ,  $5^{\circ}\text{S}$ , the equator, and  $5^{\circ}\text{N}$  listed and plotted from  $125^{\circ}\text{E}$  to  $170^{\circ}\text{E}$  or  $150^{\circ}\text{E}$  to  $170^{\circ}\text{E}$ . The full scale plot, of which this figure is a part, extends to  $80^{\circ}\text{W}$ .

MONTH 5/72

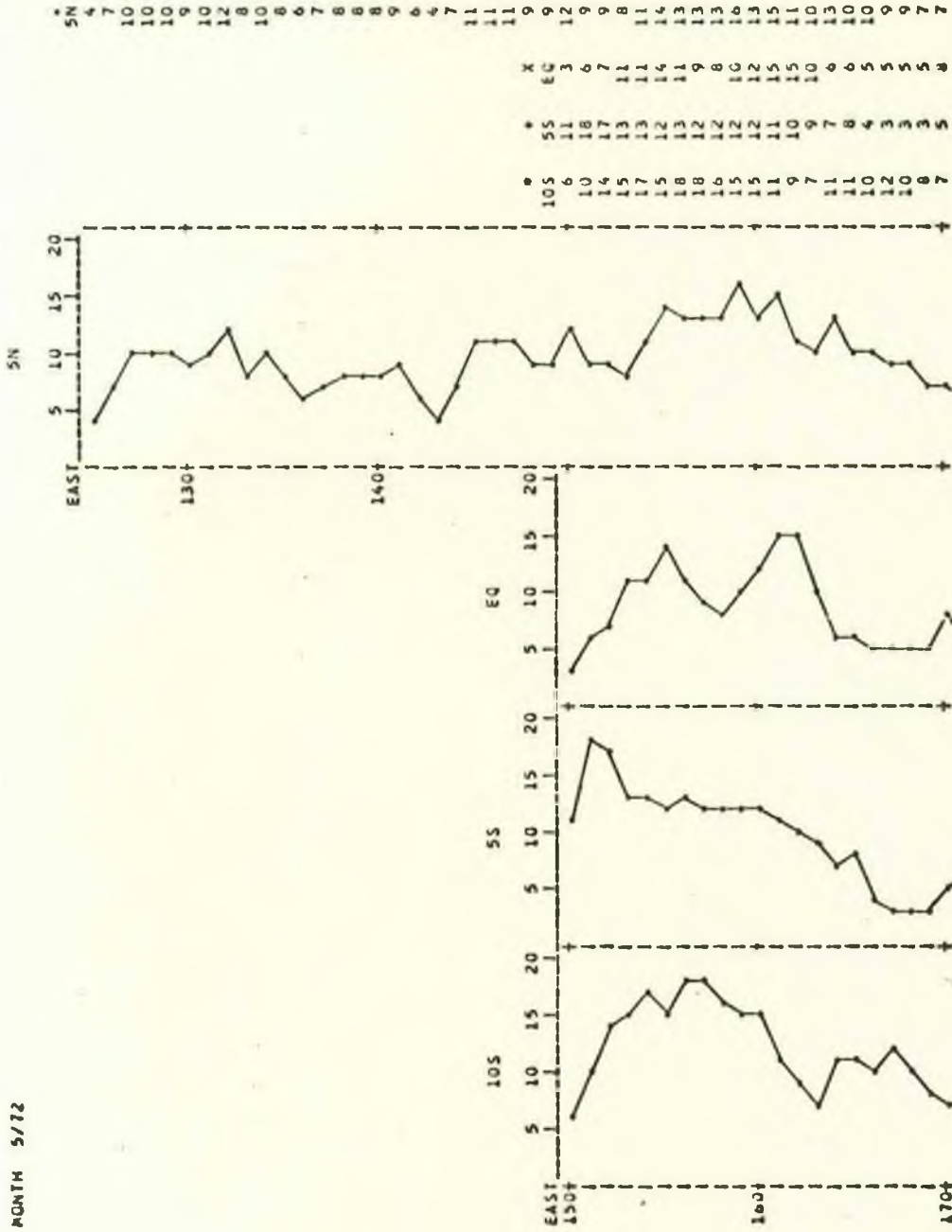


Fig. 23 Cross section,  $20^{\circ}\text{N}$  to  $20^{\circ}\text{S}$ , plotting the sum of the differences in the number of days of highly reflective cloud cover for May 1972 minus May 1971. The area of coverage is from  $125^{\circ}\text{E}$  to  $80^{\circ}\text{W}$  in the Northern Hemisphere and  $150^{\circ}\text{E}$  to  $80^{\circ}\text{W}$  in the Southern Hemisphere. The lower right-hand integer number (11692) is the sum of all the grid points in the area.

5/72 MINUS 5/71

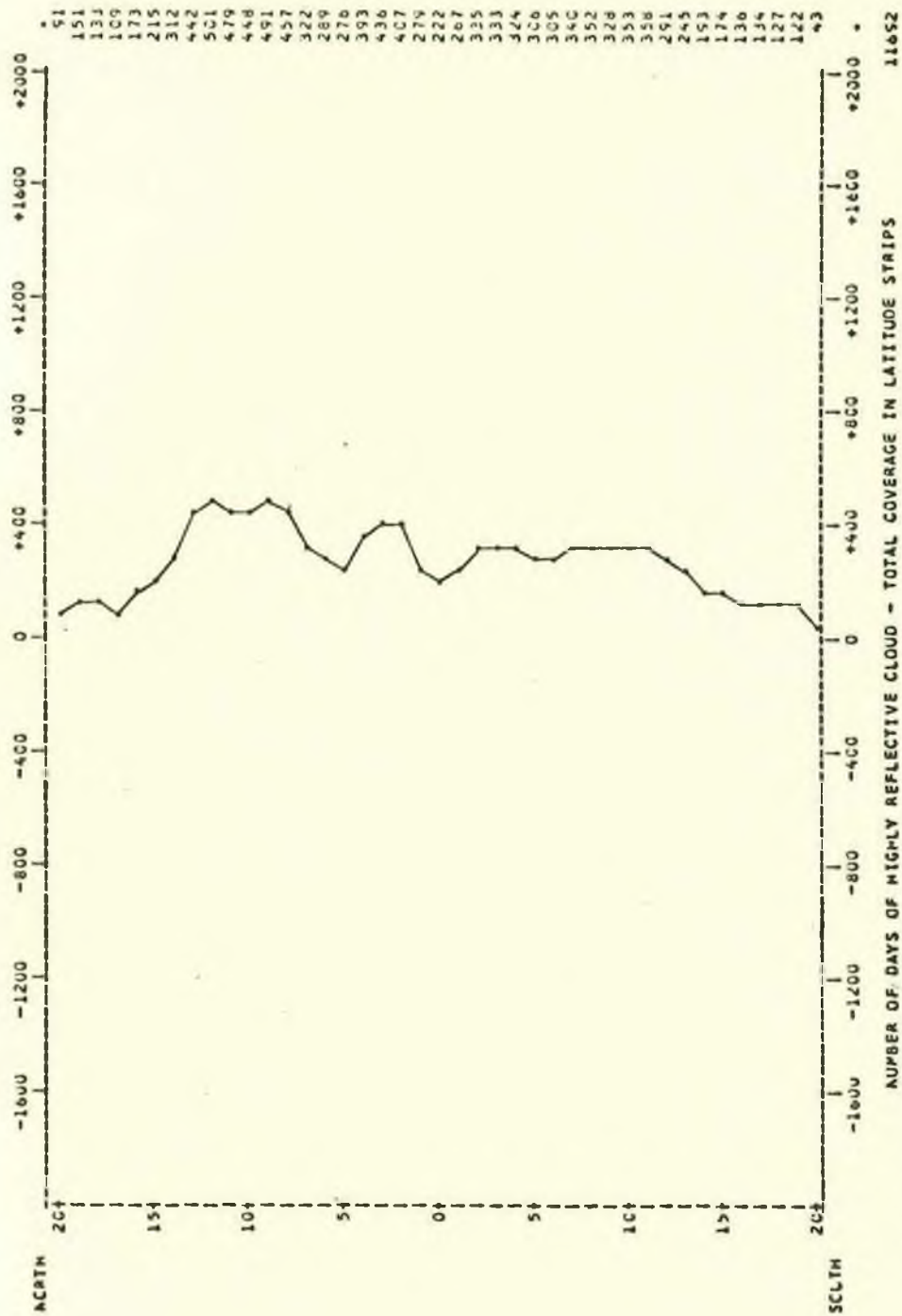


Fig. 24 Same as Fig. 23 except the cross section is now plotted for forty degree increments of the Pacific Ocean region.

5/72 MINUS 5/71



710 5071 3295 1810

Fig. 25 Cross section, 20°N to 20°S, plotting the difference in the average number of days of highly reflective cloud cover for May 1972 minus May 1971 for the area from 161°E to 160°W.

5/72 MINUS 5/71



NUMBER OF DAYS OF HIGHLY REFLECTIVE CLOUD - AVERAGE COVERAGE IN LATITUDE STRIPS

101E-160W



Fig. 26 Statistics and scatter diagram derived from equations (2.1) to (2.7) for the period May 1971 to January 1974. The vertical axis is in units of millimeters of rainfall. The horizontal axis is in units of the number of days of highly reflective cloud cover. The straight line is the least squares best fit.

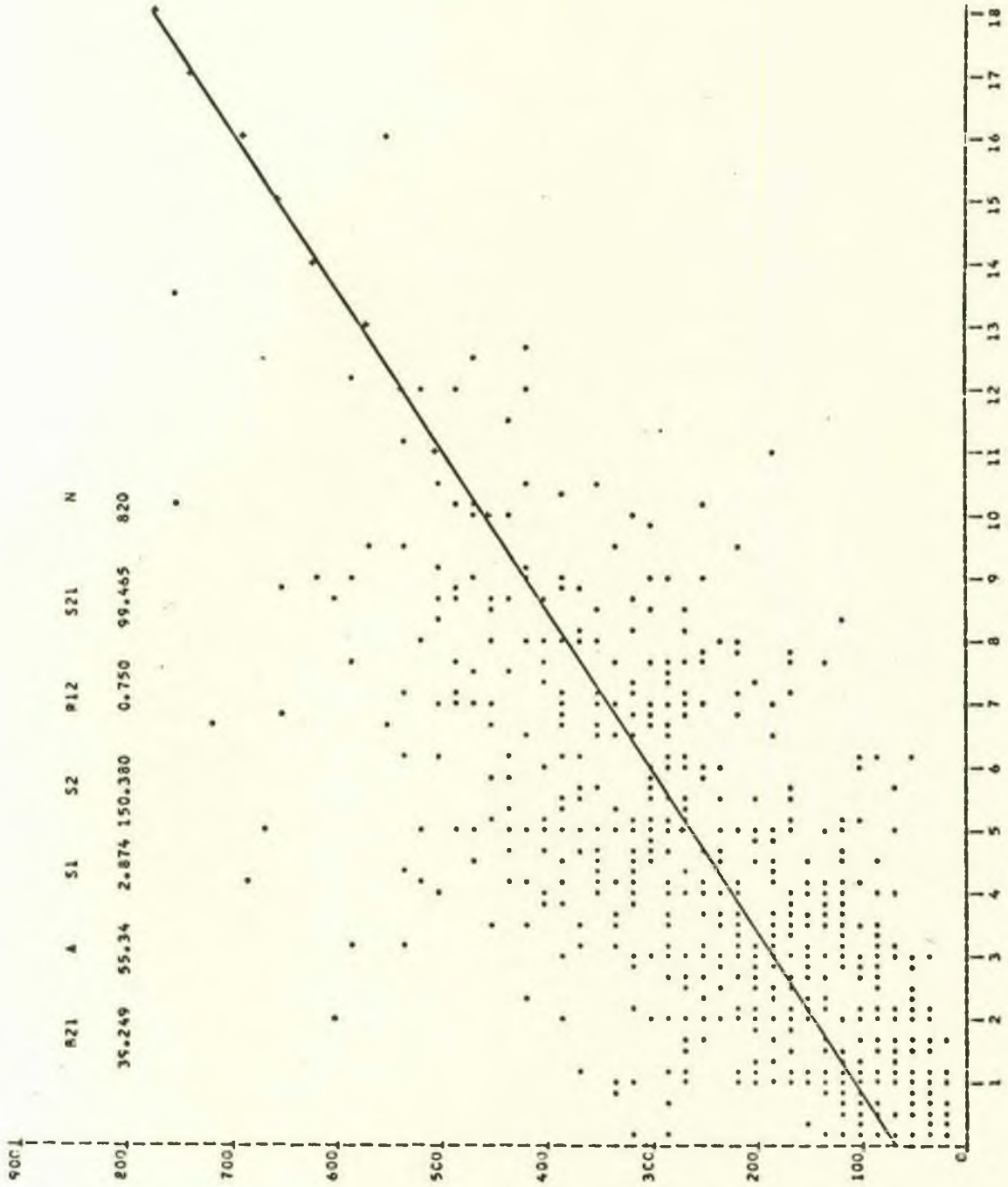
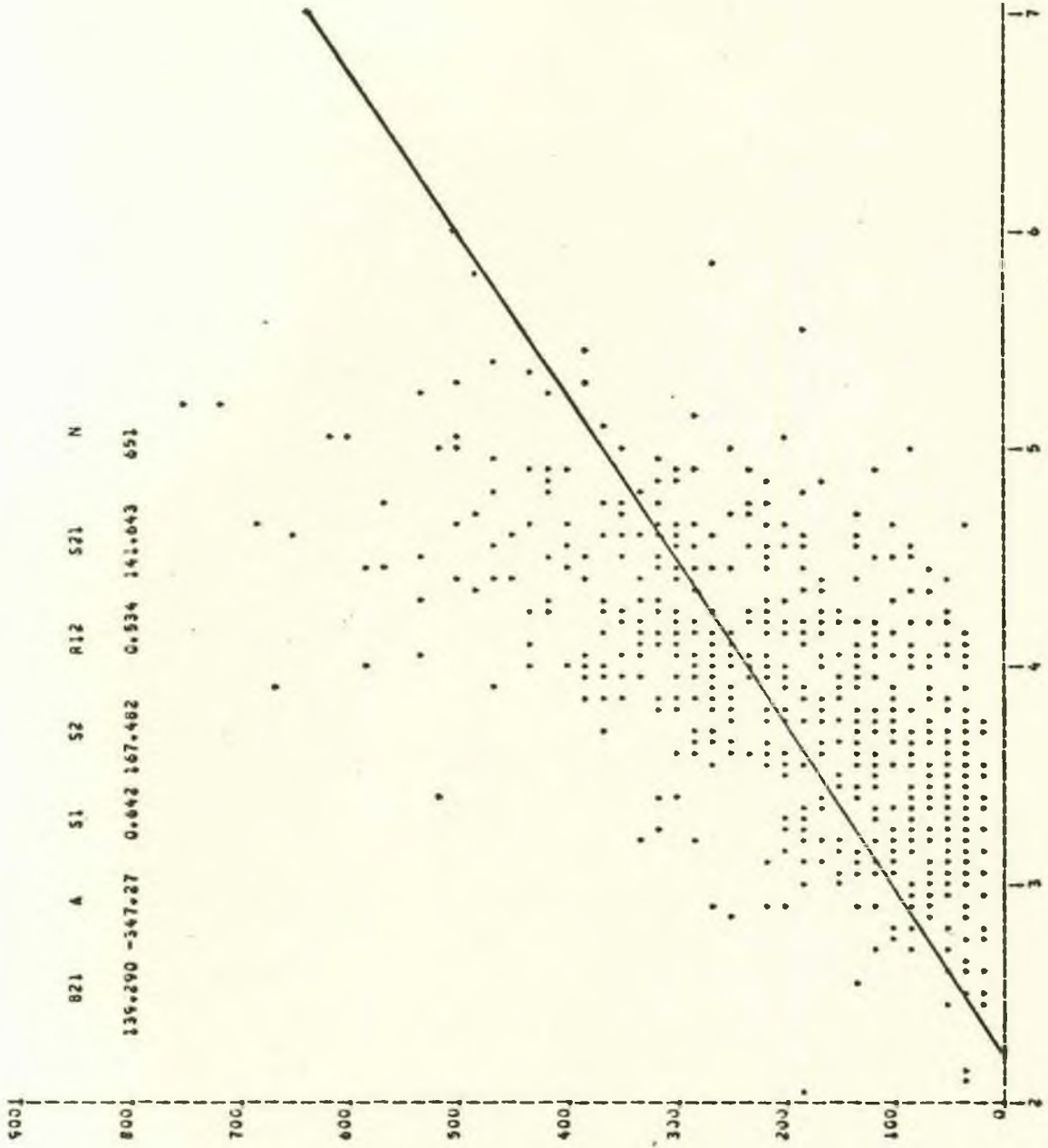


Fig. 27 Statistics and scatter diagram derived from equations (2.1) to (2.7) for the period May 1971 to January 1974. The vertical axis is in units of millimeters of rainfall. The horizontal axis is in oktas. The straight line is the least squares best fit.



821 A S1 S2 R12 S21 N  
 135.290 -347.27 0.642 167.482 0.534 141.043 651

Fig. 28 Cross section, 20°N to 20°S, plotting five estimations of the annual precipitation in centimeters for the Pacific Ocean. The estimate derived from highly reflective cloud is plotted as the "HRC" estimate. The right-most column of numbers is the annual precipitation estimates derived from highly reflective cloud for each latitude.

PACIFIC OCEAN

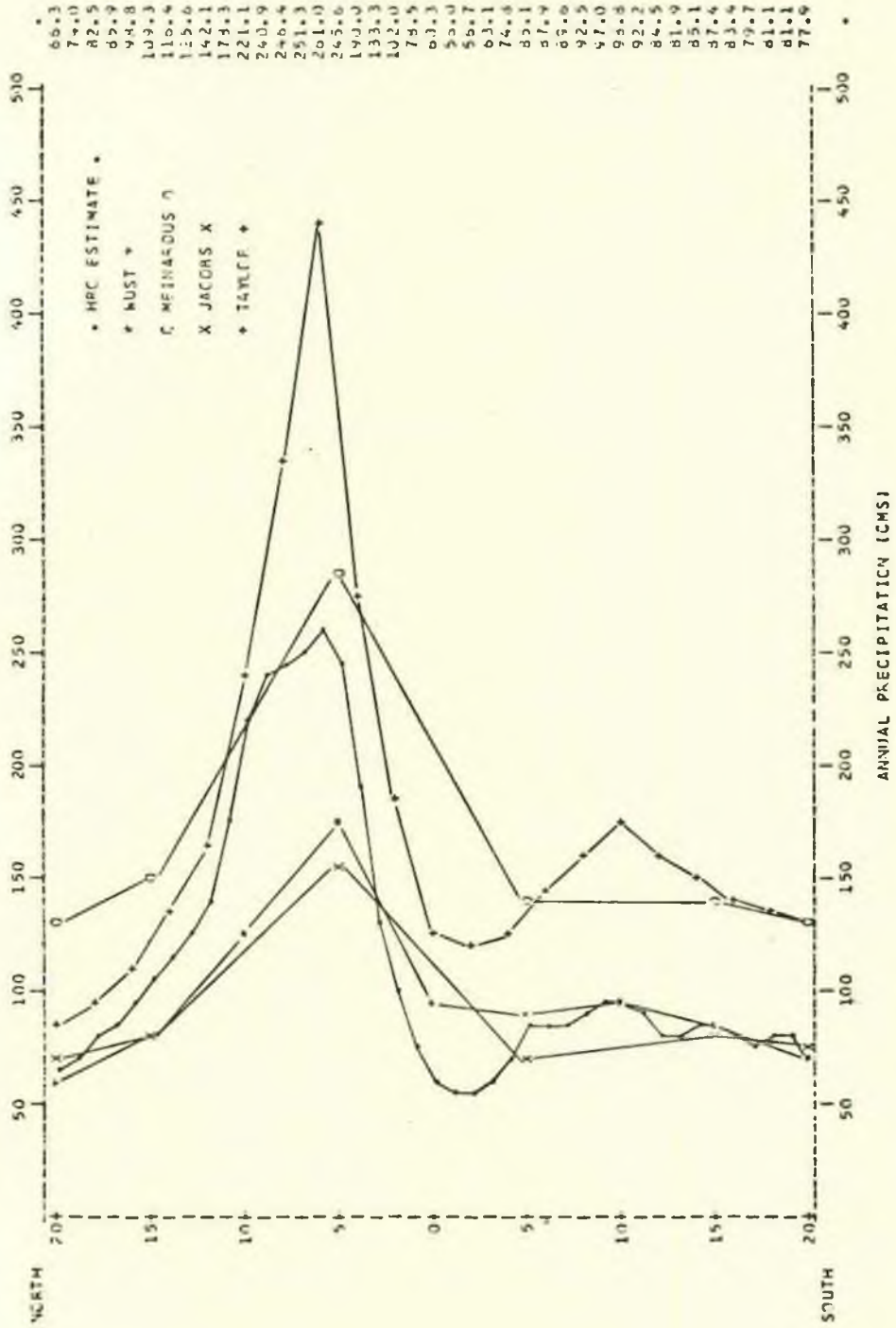
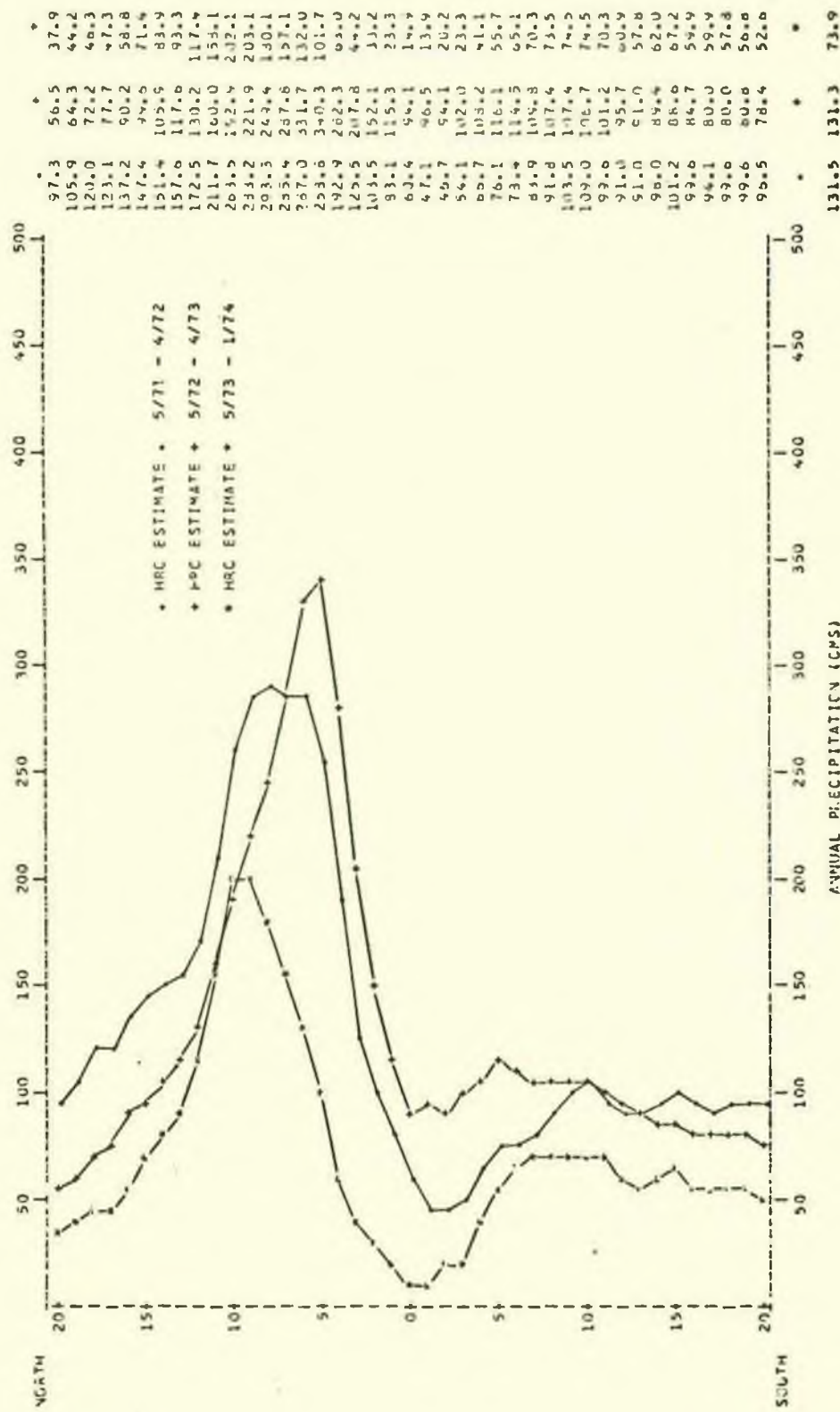


Fig. 29 Cross section, 20°N to 20°S, showing the annual precipitation in centimeters for the Pacific Ocean. Three periods are shown; May 1971 to April 1972, May 1972 to April 1973, and a 12 month extrapolation of May 1973 to January 1974.

PACIFIC OCEAN



\* HRC ESTIMATE \* 5/71 - 4/72  
 + P-PC ESTIMATE + 5/72 - 4/73  
 \* HRC ESTIMATE \* 5/73 - 1/74

ANNUAL PRECIPITATION (CPS)



## APPENDIX

## A. Station List

## A. PACIFIC ISLAND RAINFALL STATIONS

FA--indicates station on flat atoll.

RA--indicates station on raised atoll with elevation given in meters in the following parentheses.

	<u>Station</u>	<u>Latitude-Longitude</u>		<u>Type</u>
1.	ARORAE	00 12 N	173 37 E	FA
2.	ATAFU	08 32 S	172 31 W	FA
3.	BERU	01 21 S	175 58 E	FA
4.	BUTARITARI	03 07 N	172 48 E	FA
5.	CANTON	02 46 S	171 43 W	FA
6.	CHRISTMAS	01 59 N	157 22 W	RA (12)
7.	ENIWETOK	11 20 N	161 21 E	FA
8.	FANNING	03 51 N	159 22 W	FA
9.	FUNAFUTI	08 31 S	179 12 E	FA
10.	HAO	10 06 S	141 02 W	FA
11.	HEREHERETUE	19 54 S	145 04 W	FA
12.	JOHNSTON	16 44 N	169 31 W	RA (21)
13.	KAPINGAMARANGI	01 05 N	154 48 E	FA
14.	KWAJALEIN	08 44 N	167 43 E	FA
15.	LITTLE MAKIN	03 18 N	173 08 E	FA
16.	MAJURO	07 05 N	171 23 E	FA
17.	MANIHIKI	10 26 S	161 01 W	FA
18.	MOKIL	06 41 N	159 47 E	FA
19.	MOPELIA	16 55 E	154 00 W	FA
20.	NANUMANGA	06 19 S	176 20 E	FA
21.	NANUMEA	05 39 S	176 06 E	FA

22.	NONOUTI	00 40 S	179 20 E	FA
23.	NORTH TABITEUEA	01 10 S	174 45 E	FA
24.	NUI	07 16 S	176 10 E	FA
25.	NUKUFETAU	08 04 S	178 20 E	FA
26.	NUKUORO	00 03 N	155 01 E	FA
27.	PALMERSTON	18 04 S	163 10 W	FA
28.	PENRHYN	09 01 S	158 03 W	FA
29.	PUKA PUKA	10 53 S	165 49 W	FA
30.	RAKAHANGA	10 03 S	161 06 W	FA
31.	SATAWAN	04 18 N	152 42 E	FA
32.	SWAIN	11 03 S	171 05 W	FA
33.	TAKAROA	14 29 S	145 02 W	FA
34.	TAMANA	02 29 S	175 58 E	FA
35.	TARAWA	01 21 N	172 56 E	FA
36.	ULITHI	10 02 N	139 48 E	FA
37.	WAKE	19 17 N	166 39 E	FA
38.	WASHINGTON	04 44 N	160 25 W	FA
39.	WILLIS	16 18 S	149 59 E	FA
40.	WOLEAI	07 22 N	143 55 E	FA

## REFERENCES

- Barrett, E. C., (1970). The estimation of monthly rainfall from satellite data. Mon. Wea. Rev., 98, pp. 322-327.
- Blumenstock, D. I., and S. Price, (1967). Climates of the States, Hawaii. U. S. Department of Commerce, Washington, D. C., 27 pp.
- Haurwitz, B., and J. M. Austin, (1944). Climatology. New York, McGraw-Hill, 410 pp.
- Jacobs, W. W., (1951). Energy exchange between sea and atmosphere. Bull. Scripps Inst. Oceanog. Univ. Calif., Vol. 6, pp 27-122.
- Meinardus, W., (1934). Eine neue Niederschlagskarte der Erde. Peterm. Geogr. Mitt., Vol. 80, pp. 1-4.
- Panofsky, H. A., and G. W. Brier, (1968). Some Applications of Statistics to Meteorology. Pennsylvania, Pennsylvania State University, 224 pp.
- Riehl, H., (1954). Tropical Meteorology. New York, McGraw-Hill, 392 pp.
- Sadler, J. C., (1969). Average cloudiness in the tropics from satellite observations. International Indian Ocean Expedition Meteorological Monographs No. 2, Honolulu, East West Center Press, 22 pp.
- Schott, G., (1935). Geographie des Indischen und Stillen Ozeans. Hamburg, C. Boysen, 413 pp.
- Stidd, C. D., and L. B. Leopold, (1951). The geographic distribution of average monthly rainfall, Hawaii. Meteorological Monographs, Vol. 1, No. 3, pp. 24-33.
- Taylor, R. C., (1973). An atlas of Pacific island rainfall. Data Report No. 25, Office of Naval Research, CONTRACT NO. N00014-70-A-0016-0001, 5 pp.
- Wuest, G., (1936). Landerkundliche Forschung. Festschrift Norbert Krebs, pp. 347-359.